Evaluation of Aerosol Production Potential of Type Surfaces in Arizona

by

W.G. Nickling

J.A. Gillies

SEP 1986
OFFICE OF AIR QUALITY
MANAGEMENT

Submitted to

Engineering–Science
125 W. Huntington Drive
Arcadia California

for

EPA Contract No. 68-02-388

INTRODUCTION

During the past decade, considerable interest has been focused on the emission, transport, deposition and climatological effects of natural and anthropogenic aerosols (e.g. Gillette et al. 1982; 1978; Deluisi et al. 1977; Pewe, 1981). Several studies have also considered the effects of mass particle concentration on light extinction (Pilat and Ensor, 1971), climate (Idso and Brazel, 1974), human health hazards (Leathers, 1981), visibility (Patterson and Gillette, 1977b) and ambient air quality (Hagen and Woodruff, 1973). In addition a large volume of literature has developed on the atmospheric, textural and surface conditions which interact to produce atmospheric aerosols.

Despite this, few studies have attempted to identify and classify, in a quantitative manner, the relative aerosol production potential of natural and anthropogenic surfaces. Information of this nature is needed in our understanding total suspended particulate loadings especially in areas such as the U.S. Southwest where dust storm frequencies and T.S.P. loadings are relatively high (Nickling and Brazel, 1984; Brazel and Nickling, 1986). Moreover, the recent decision by the Environmental Protection Agency to modify the current T.S.P. standards to a limitation based on particulates having a mass mean aerodynamic diameter of less than 10 micrometres, requires a better knowledge of the potential sources and land-use activities which result in high aerosol fluxes so that appropriate environmental standards can be established.

In order to evaluate the aerosol production potential of various surface types, field wind tunnel tests were carried out at 13 sites in

Arizona during May and June 1986. The selected sites are representative of both undisturbed and disturbed surfaces that are typical of large land areas in the state. The selected sites included: disturbed and undisturbed scrub desert, fluvial channels, active and abandoned agricultural fields as well as mine tailings.

The following report presents the results of the study including a brief discussion of the factors affecting the entrainment and transport of particulates.

THE ENTRAINMENT AND TRANSPORT OF PARTICULATES

The Wind Profile

The wind shear near the ground has a direct influence on the suspension or resuspension of soil particles. It is well established that a wind strong enough to cause the movement of soil is always turbulent. The change in velocity with height in the turbulent boundary layer above a non-eroding surface is traditionally described by a logarithmic equation first proposed by Schmidt (1925) and Prandtl (1932). This equation has the form

$$u_z = (u_*/k) \ln(z/z_o) \qquad \ldots 1$$

in which u_z is the average horizontal velocity at a height z above the surface, k is the von Karman constant having a value of 0.4, z_o is the roughness length, and is the height above the surface where the wind velocity is zero. The zero-velocity plane is not obvious from an inspection of the ground surface, but is estimated by plotting the velocity above the ground against the height above the average ground surface on an arithmetic

scale and projecting the curve to the ordinate.

The parameter u_* is known as the friction velocity and is an index of the rate of increase of velocity with height. The stronger the wind, the greater u_*. The friction velocity is defined by the equation

$$\tau/\rho = u_*^2 \qquad \ldots 2$$

where τ is the shearing stress at some height z above the surface and ρ is the air density.

Above an eroding soil surface the velocity gradient undergoes a significant change in which Eq. 1 does not strictly apply. Bagnold (1936) and Chepil and Milne (1941) were the first to show that sand and soil movement in saltation reduces the momentum and, therefore, the surface velocity of the wind (see Fig. 1). This figure is reproduced from Chepil (1940) and represents data obtained from a portable wind tunnel designed for use in the field. The solid lines indicate velocity gradients obtained over a surface which was "fixed" by spraying it with water. The dashed lines indicate the velocity gradient over the same soil surface with soil movement in progress. Note that an eroding soil surface reduces wind velocities to a considerable height. Chepil (1940) shows that the wind profile under eroding conditions conforms to the equation

$$u_z = 5.75\ u_*' \log(z/k') + u_t \qquad \ldots 3$$

in which u_z is the velocity at height z, u_*' is the drag velocity above an eroding surface, k′ is the height above z_o to which all drag velocity curves merge and u_t is the velocity at height k′. Chepil found that, within the limitations of his data, u_t remained constant independent of the wind speed.

It is evident from Fig. 1 that the higher the drag velocity u_* (i.e.

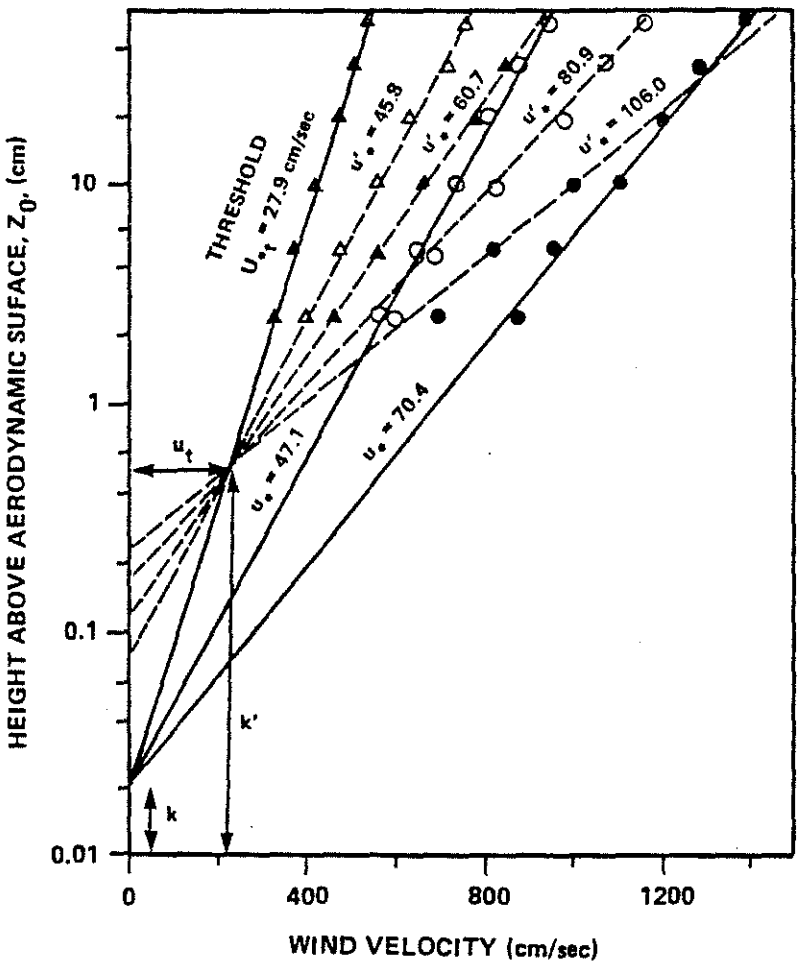
HEIGHT ABOVE AERODYNAMIC SUFACE, $Z_{0'}$ (cm)
10
1
0.1
0.01
0
400
800
1200
WIND VELOCITY (cm/sec)
THRESHOLD
U_{*t} = 27.9 cm/sec
u'* = 45.9
u'* = 60.7
u'* = 80.9
u'* = 106.0
u* = 47.1
u* = 70.4
u_t
k'
k

Figure 1

the stronger the wind blows) the lower is the velocity below the height k'. This condition arises because of the larger concentrations of saltating soil grains in the stronger winds which tend to lower the wind velocity below the height k'. Chepil and Milne (1941) found that the height k' was considerably below the average height of saltation. Owen (1964) suggests that the height of the saltation layer (δ) can be defined by

$$\delta = u_*^2/2g \qquad \ldots 4$$

Initiation of Particle Movement

The initiation of particle movement by wind has been investigated by numerous authors. The majority of this work has focused on the effects of atmospheric and textural variables, which in general control fluid threshold shear velocity by altering particle Reynolds number and/or particle fluid drag. Complimentary studies have also been concerned with the role of various interparticle forces, such as capillary water tension (Belly, 1964; Azizov, 1977), soluble salts (Gillette et al., 1980; Nickling and Ecclestone, 1981; Nickling, 1984), or cohesive forces such as electrostatic charges (Iversen and White, 1982) which tend to bond individual grains together, thereby increasing fluid threshold and decreasing the supply of grains to the airstream.

When air blows across the surface of dry loose sand a critical fluid shear stress (τ_c) must be achieved in order to initiate motion. This critical shear stress can be expressed as a function of the shear velocity (U_{*t}) of the air moving over the surface by

$$U_{*t} = \sqrt{\frac{\tau c}{\rho}} \qquad \ldots 5$$

where ρ is the density of the air. The shear velocity can be determined empirically from the wind velocity profile above the eroding surface (Eq. 1).

The critical shear velocity necessary to initiate motion has been termed the fluid threshold by Bagnold (1941) and can be expressed as

$$U_{*t} = A \sqrt{\frac{\rho p - \rho a}{\rho p} \cdot g \cdot Dp} \qquad \ldots 6$$

where ρ_p and ρ_a are the particle and air densities respectively, g acceleration due to gravity, D_p the particle diameter and A an empirical coefficient equal to approximately 0.1 for particle friction Reynolds numbers (B) > 3.5 (i.e. an equivalent grain diameter > 0.01 cm). Bagnold (1941) suggests that when particle friction Reynolds number is > 3.5 individual grains protrude into the air stream carrying the fluid drag and causing small eddies to form downwind from the particle. He also argues that for Reynolds numbers < 3.5 all particles lie below a viscous sublayer resulting in the fluid drag being distributed more evenly over the entire surface rather than being carried by a few more isolated grains. Under these conditions when particle size becomes relatively small (< 0.2 mm) the value of the coefficient A begins to rise, resulting in a sharp upturn of the threshold curve as grain size decreases (Fig. 2).

Grains initially entrained into the air stream by fluid drag may begin to bounce or saltate downwind. During the downwind movement the velocity and hence momentum of these grains is increased before they fall back to the

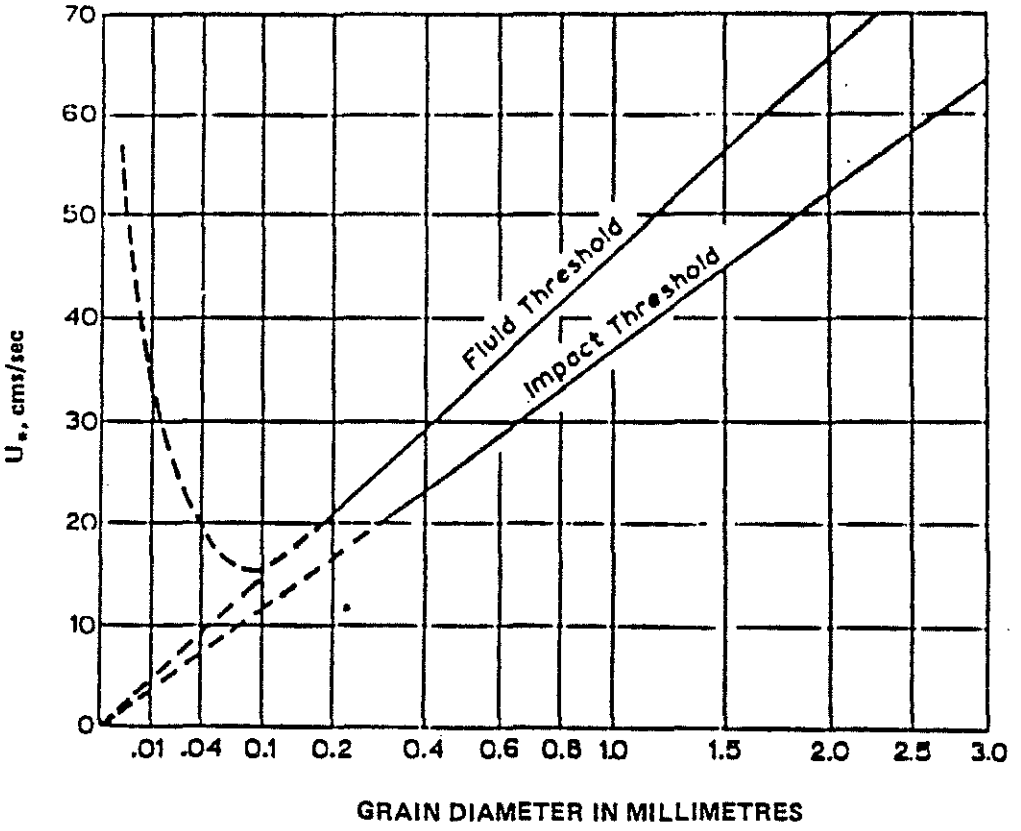
70
60
50
40
30
20
10
0
U_*, cms/sec
Fluid Threshold
Impact Threshold
.01 .04 0.1 0.2 0.4 0.6 0.8 1.0 1.5 2.0 2.5 3.0
GRAIN DIAMETER IN MILLIMETRES

Figure 2

surface. On striking the surface the moving grains may ricochet off other grains and become re-entrained or alternatively may become embedded in the surface. In both cases, momentum is transferred to the surface in the disturbance of one or more stationary grains. As a result of the impact of saltating grains, the fluid drag required to move the stationary surface grains is significantly reduced. This new, lower threshold required to move stationary grains after the initial movement of a few particles has been termed the dynamic or impact threshold (Bagnold, 1941). Wind tunnel experiments by Bagnold (1941) indicate that the dynamic threshold for a given sediment follows the same square root function as the fluid threshold (Eq. 6) but with a lower coefficient A of 0.08 instead of 0.1.

Although the threshold velocity can be closely defined for a uniform sediment size greater than 0.1 mm, it can not be defined for most natural sediments because of several complicating factors. Natural sediments, no matter how well sorted usually contain a wide range of grain sizes that cause variation in fluid and dynamic threshold (Nickling, 1986). Moreover, non-erodible roughness elements, such as vegetation, pebbles and boulders which absorb momentum being transported to the ground, decrease the momentum felt by individual soil particles thereby increasing the shear velocity required to initiate motion. Similarily other surface effects (i.e. moisture, soluble salts, organic residues and clay crusts) tend to stabilize the surface decreasing entrainment.

Entrainment of Find Grained Sediment

As indicated in Bagnold's (1941) threshold curve, the shear velocity (u_*) required to entrain particles < 0.1 mm increases rapidly as grain size decreases negating the use of Eq. 6 for threshold determinations. Bagnold (1941) suggested that this results from the fact that particles in this size range are too small (i.e. low particle friction Reynolds number) to protrude above the laminar sublayer close to the surface.

Miller and Komar (1977) and Iversen et al. (1976) however, suggest that the upturn in the threshold curve may be more directly controlled by interparticle cohesive forces (i.e. moisture films, van der Waal's forces, and electrostatic charges) rather than by Reynolds number effects. In support of this argument Iversen et al. (1976) and Iversen and White (1982) have developed and tested modified threshold equations which take into account interparticle forces for small grains. Their detailed wind tunnel data also indicate that the variation in threshold shear velocity for small particles is a function of particle size distribution and particle density.

Iversen et al. (1976) argue that the forces on an erodible particle include the drag D, the lift L, the aerodynamic overturning moment M, the weight W and an interparticle force I_p. At the threshold condition the particle forces are assumed to be in equilibrium about the point P. Thus, the moments about the point P are:

$$Da + Lb + M = Wb + I_p c$$

Based on this assumption Iversen et al. (1976) derive an expression for U_{*t}

of the form

$$u_{*t} = A_1 \left[\frac{\rho_p \, gD_p}{\rho} \left[\frac{1 + A_4 I_p / \rho_p gD_p^3}{1 + A_3 B} \right] \right]^{1/2} \quad \ldots 8$$

The coefficients A_1, A_3, A_4 are unknown, but have been approximated using an empirical set of values derived from detailed wind tunnel tests. Using these values and assuming that the interparticle force, I_p, is proportional to a power of the particle diameter they derive the following expression for

$$u_{*t} = 0.174 \left[\frac{\rho_p gD_p}{\rho} \left[\frac{1 + 0.0314 (D_p)^{0.837} / \rho_p gD_p^3}{1 + 0.588B} \right] \right]^{1/2} \quad \ldots 9$$

where the constant 0.0314 has the units of $g.cm^{0.163}/sec^2$ and B is the particle friction Reynolds Number. This relationship has been more thoroughly tested by Iversen and White (1982) and McKenna-Neuman (1984) and appears to adequately describe and predict the observed upturn in Bagnold's (1941) threshold curve for small particles.

The rapid increase of threshold shear velocity with decreasing size for small particles is of considerable importance when one considers the entrainment of fine grained sediment under natural wind conditions.

Patterson and Gillette (1977a), based on field studies, suggest that particles transported long distances typically have particle diameters ranging from 0.1 to 20 μm. Using the Iversen et al. (1976) threshold equation the threshold shear velocity (u_{*t}) required to entrain a 20 μm particle is approximately 34 cm/s which corresponds to a wind velocity of 35 km/h (22 mph) at 10 m if a logarithmic wind profile is assumed. In contrast the threshold shear velocity of a 1.0 μm particle is 180 cm/s which is

equivalent to a 10 m wind speed of 190 km/h. Thus, for very small particles (<10 μm) it is unlikely that they can be entrained by the direct force of the wind under normal meteorological conditions. The relative immobility of fine particles has been noted by many authors in both field and laboratory wind tunnel experiments. In almost all cases these authors conclude that it is the saltation of larger particles impacting the surface that is the dominant mechanism by which suspended particles are ejected into the airstream and not the direct action of the wind.

Threshold Velocity of Natural Sediments

The work of Bagnold (1941), Chepil (1950) and Iversen *et al*. (1976) has greatly increased our understanding of the threshold velocities required for the initiation of particulate movement in simple soil systems. However, relatively little is known regarding the thresholds of natural soils. The most extensive work to date is that of Gillette *et al*. (1980; 1982) who have investigated the threshold velocities required to entrain particles for a variety of undisturbed and disturbed desert soils. Their work indicates that natural soils have considerably higher threshold velocities than those predicted by traditional models because of the grain size distributions, presence of surface roughness elements, surface moisture effects and the presence of surface crusts caused by variation in mineralogy, clay content and precipitated salts. In general, they found that threshold velocity for the studied soils correlated negatively with percentage of sand and positively with increasing percentage and size of aggregates and particles > 1 mm. Their results also clearly demonstrate that surface disturbance

Table 1. Summary of Soil Characteristics and Threshold Velocities (Gillette et al., 1980)

GROUP	NUMBER	GEOMORPHOLOGICAL SETTING	DESCRIPTION	CRUSTAL HARDNESS	CRUSTAL THICKNESS (cm)	ROUGHNESS HEIGHT z_o (cm)	MODE OF DRY AGGREGATE SIZE (μm)		THRESHOLD VELOCITY (cm/s)	
							UNDISTURBED	DISTURBED	UNDISTURBED	DISTURBED
I Salt Crusts	1	Center of playa	Hard salt crust with moist soil below.	Hard	0.6	0.18	>100,000	Wet	>250(NR)[a]	NR
II Desert Pavements	1	Alluvial stream deposit	Fine desert pavements, no varnish, not mature.	Slightly hard-hard	2.5	0.4	15,000	66	271	66
	2	Alluvial stream deposit	Coarse desert pavement, no varnish, not mature.	Slightly hard-hard	2.5	0.48	15,000	66	278	66
	3	Alluvial fan	Mature, varnished desert pavement, rounded cobbles.	Slightly hard	2.5	0.04	35,000	175	154	59
	4	Alluvial fan	Immature pavement, no varnish.	Slightly hard	2.5	0.15	35,000	175	163	42
III Crusted Soils	1	Center of playa	Cracked, curled clay crust.	Hard	1.3	0.19	35,000	15,000	>285(NR)	182
	2	Center of playa	Cracked, curled clay crust.	Hard	2.5	0.24	15,000	1,500	>339(NR)	158
	3	Edge of playa	Silty crust.	Slightly hard	1.3	0.006	35,000	100	>154(NR)	40
	4	Edge of playa	Smooth crust.	Slightly hard	0.5	0.006	15,000	750	265	29
	5	Edge of playa	Clay crust broken into 2-5 mm pellets.	Extremely hard	0	0.002	15,000	750	204	35
	6	Center of playa	Thin peels of clay on thick flat crust.	Slightly hard	3.8	0.016	>100,000	275	>230(NR)	36
	7	Flat near playa	Silty soil near desert road.		0	0.01	...	375		35
	8	Center of playa	Thick, hard clay crust, no cracks.	Extremely hard	2.5	0.01	>100,000	175	>191(NR)	35
	9	Edge of playa	Silty crust, more easily broken than at center of playa.	Slightly hard	1.9	0.005	15,000	750	>200(NR)	27
	10	Center of playa	Cracked clay crust.	Slightly hard	0.6	0.016	15,000	4,850	>300(NR)	51
	11	Center of playa	Hard clay crust; narrow cracks.	Very hard	0.6	0.016	35,000	375	>317(NR)	101
	12	Edge of playa	Curled clay peels on hard clay crust.	Slightly hard	0.08	0.004	3,000	175	121	33
	13	Center of playa	Hard clay crust; narrow cracks.	Slightly hard	1.3	0.008	35,000	3,000	>339(NR)	88
	14	Center of playa	Hard clay crust; narrow cracks.	Hard	2.5	0.00003	35,000	1,500	>222(NR)	19
	15	Prairie, flat	Thin clay crust; flat and soft.	Slightly hard	0.3	0.3	35,000	750	261	83

[a] NR means Threshold Velocity not reached.

Continued -----

Table 1. Summary of Soil Characteristics and Threshold Velocities (Gillette et al., 1980) - continued.

GROUP	NUMBER	GEOMORPHOLOGICAL SETTING	DESCRIPTION	CRUSTAL HARDNESS	CRUSTAL THICKNESS (cm)	ROUGHNESS HEIGHT z_o (cm)	MODE OF DRY AGGREGATE SIZE (μm)		THRESHOLD VELOCITY (cm/s)	
							UNDISTURBED	DISTURBED	UNDISTURBED	DISTURBED
IV Other Soils	1	Aeolian deposit on a fan; thin coating of grus.	Near mountains; fine sand under thin layer of grus.	Soft	0.6	0.35	375	750	191	43
	2	Aeolian deposit on alluvial fan; thin coating of grus.	Lower of fan; fine sand under thin layer of grus.	Soft	0.6	0.06	175	375	147	33
	3	Lower alluvial fan near playa	Vesicular crust; sandy soil.	Slightly hard	1.3	0.009	375	375	146	26
	4	Flat, Prairie	Loose, sandy soil		0	0.0005	750	175	...	26
	5	Flat, Prairie	Loose, loamy fine sand		0	0.0006	1,500	175	...	25
	6	Sand dune	Sand dune with very soft crust.	Soft	0.6	0.01	1,500	750	40	28
	7	Sand dune	Sand dune with very soft crust.	Soft	0.6	0.01	1,500	750	59	34
	8	Alluvial fan	Gravel cover.	Soft	0.3	0.003	1,500	375	31-56[b]	44
	9	Alluvial fan	Gravel cover.	Soft	1.3	0.02	3,000	1,500	134-237[b]	89
	10	Desert flat	Gravel cover.	Soft	1.3	0.04	175	375	78	72
	11	Desert flat	Gravel cover.	Hard	1.3	0.001	750	375	67	31
	12	Dry wash	Gravel, thick loose layer.	Soft	0.6	0.04	750	75	89	64
	13	Desert flat	Gravel cover.	Slightly hard	1.3	0.03	3,000	375	75	40
	14	Alluvial fan	Gravel cover.	Soft	0.3	0.003	750	750	57-73[b]	47
	15	Pediment	Gravel cover.		0	0.001	...	1,500	...	50
	16	Dry wash		Soft	0.6	0.006	750	750	61	47
	17	Flat	Gravel cover.	Soft	2.5	0.04	375	375	80	61
	18	River bottom	Gravel bed.		0	0.02	...	1,500	...	60

[b] Some tests were done in several nearby locations. Ranges are given for those tests.

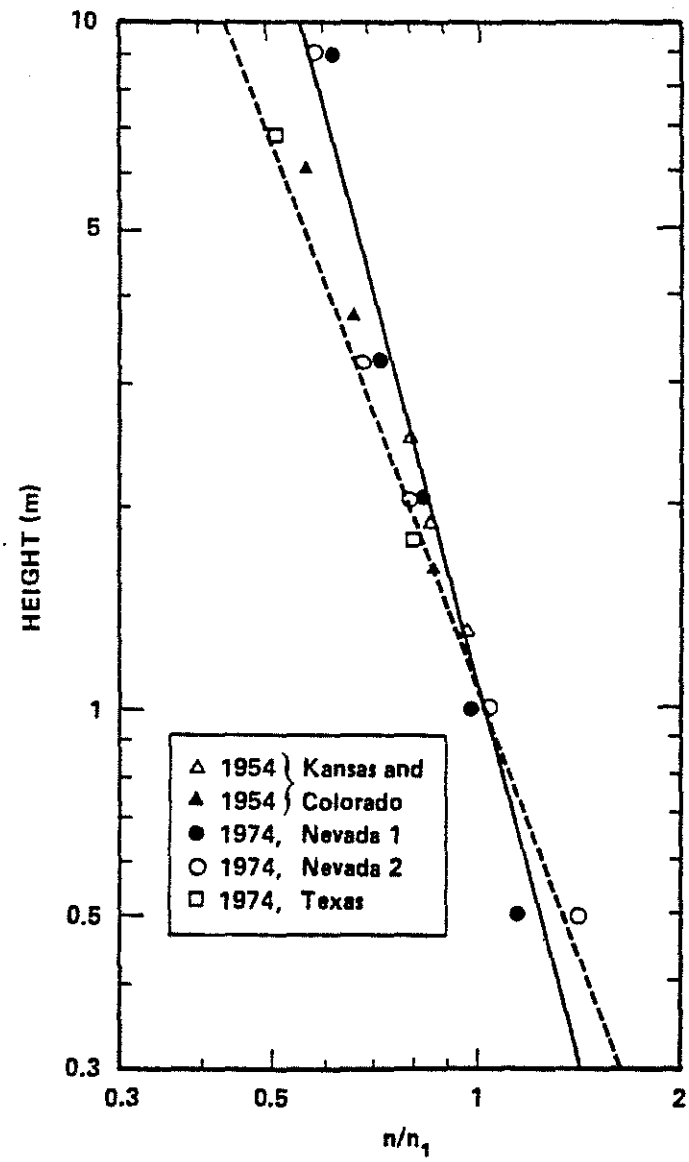
10
5
1
0.5
0.3
HEIGHT (m)
0.3
0.5
1
2
n/n1
1954 Kansas and
1954 Colorado
1974, Nevada 1
1974, Nevada 2
1974, Texas

Figure 3

and Shinn et al. (1976). It is evident that all profiles fit a power law with an exponent ranging between -0.25 and -0.35. Similar results have also been reported by Gillette (1977) and Nickling (1978).

Gillette et al. (1972) and Shinn et al. (1976) suggest that the established power-law relationship found in the concentration profiles allows the vertical dust flux, F, to be described by

$$F = K\, dn/dz \qquad \ldots 10$$

where z is height and K is the eddy diffusivity. Under neutral conditions

$$K = U_{*}kz \qquad \ldots 11$$

where K is the von Karman constant (= 0.4).

Assuming the dust concentration follows a power-law distribution

$$dn/dz = P\, n/z \qquad \ldots 12$$

where P = -0.3 (the average slope of the normalized concentration vs. height relationship).

Combining Eq. 10, 11 and 12 gives

$$F = kPU_{*}n \qquad \ldots 13$$

which can be used to calculate the vertical aerosol flux (F) from a point concentration. It should be noted however, that the saltation process directly affects the magnitude of n (Gillette, 1977; Nickling 1978) and thus is directly affected by surface textural properties, surface roughness elements, moisture content and the presence of surface crusts.

The most detailed vertical aerosol flux data available is that

presented by Gillette (1977). In this study tests were conducted over a three year period on relatively flat fields consisting of erodible soils with uniform textures. Aerosols were collected using specially designed membrane filter samples (Gillette et al. 1974) placed at heights of 1.5 and 6.0 m or 1.0 and 6.8 m. Mean wind velocity was measured at the same heights using cup anemometers.

The observed particle fluxes (F) as a function of shear velocity (U_*) for nine sites are shown in Fig. 4. The sandy soils show a fairly uniform trend of increasing vertical particle flux with shear velocity. In contrast, the loamy soils show a greater scatter in F, most likely because of their widely different dry aggregate structures. The relatively low values of vertical particle flux associated with the clay soil results from its high threshold shear velocity and the resistance of aggregates to break-up due to the presence of montmorillinitic clay.

On the assumption that the production of aerosols is related to the total horizontal soil flux, Gillette (1977) also measured the movement of soil in saltation and creep using a modified Bagnold type catcher. To compare the horizontal soil fluxes (q') with the vertical dust fluxes (F), Gillette (1977) plotted the ratio F/q' against shear velocity (U_*). The results are reproduced in Fig. 5. As can be seen little relationship exists between the ratio F/q' and U_*. The sandy soils in particular show no trend between the two parameters. There is however, a pronounced increase in F/q' with U_* for the loamy soils which is proportional to U_*. It is also evident that the ratio F/q' is very low for the clay soil which results from the high resistance of this soil to abrasion.

Although it would seem logical to suppose a relationship between the

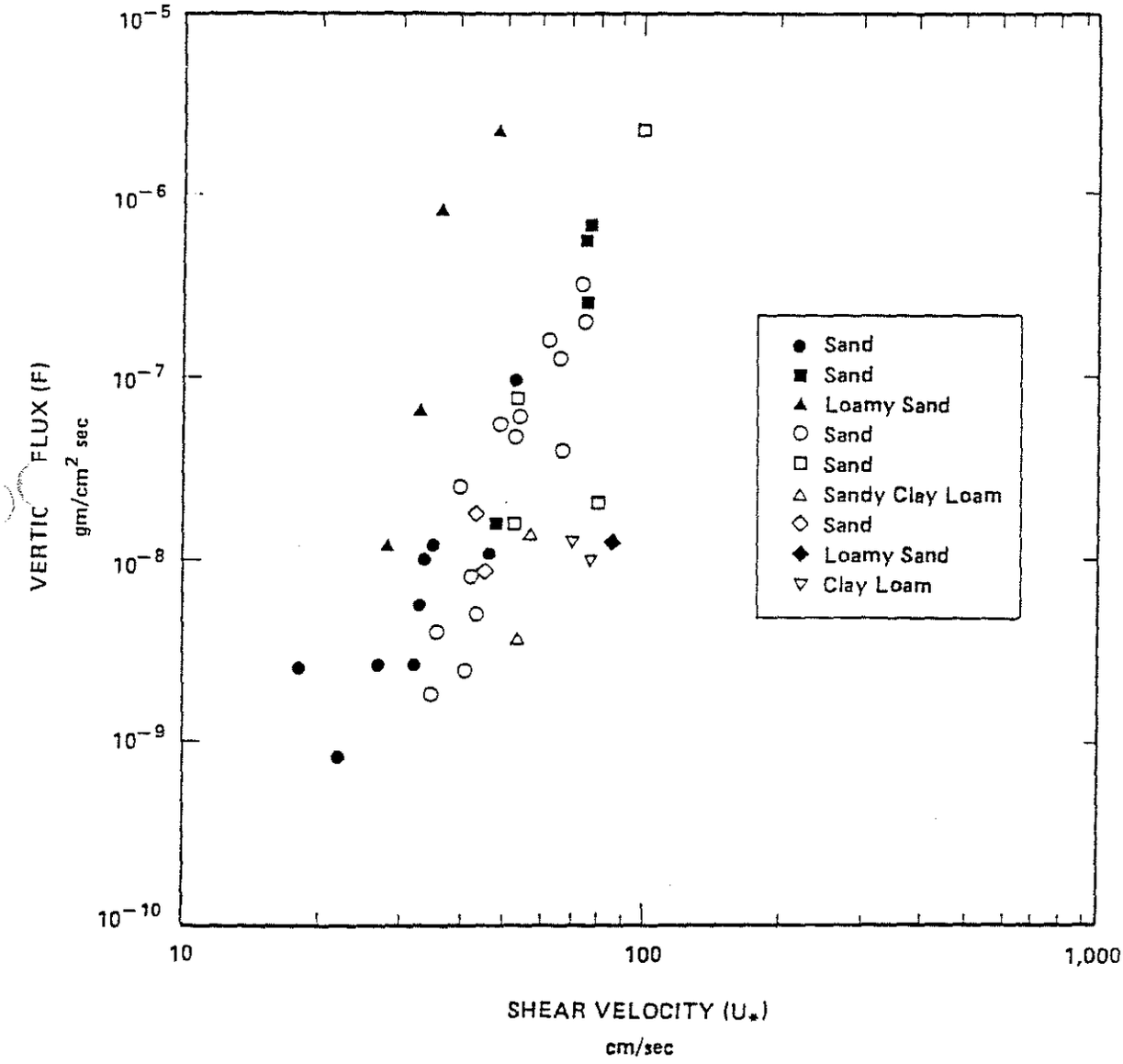
VERTIC FLUX (F)
gm/cm² sec
10⁻⁵
10⁻⁶
10⁻⁷
10⁻⁸
10⁻⁹
10⁻¹⁰
10
100
1,000
SHEAR VELOCITY (U*)
cm/sec
Sand
Sand
Loamy Sand
Sand
Sand
Sandy Clay Loam
Sand
Loamy Sand
Clay Loam

Figure 4

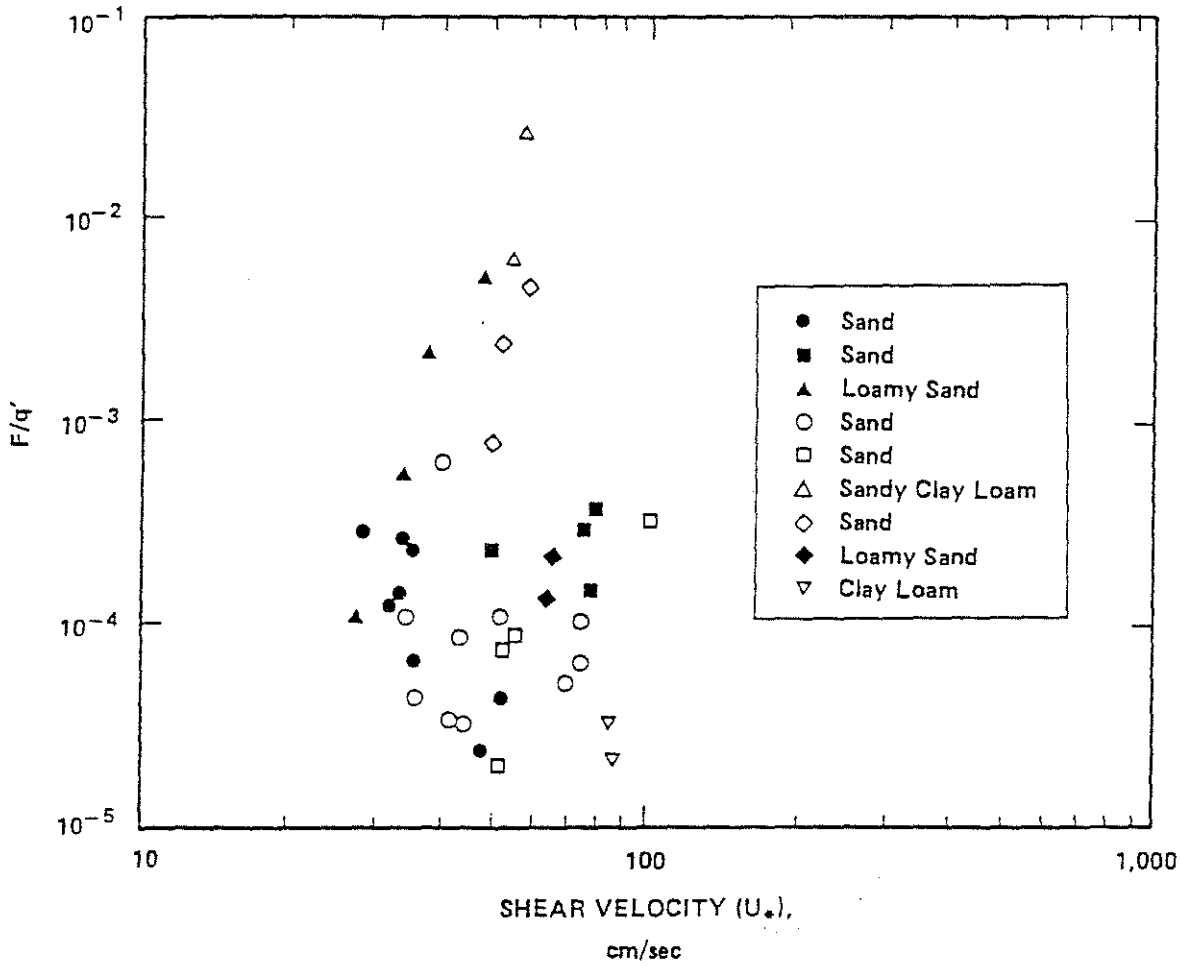
10^{-1}
10^{-2}
10^{-3}
10^{-4}
10^{-5}
F/q'
10
100
1,000
SHEAR VELOCITY (U_*),
cm/sec
Sand
Sand
Loamy Sand
Sand
Sand
Sandy Clay Loam
Sand
Loamy Sand
Clay Loam

vertical dust flux and horizontal soil movement in saltation, the relationship is not a simple one as is clearly indicated in Fig. 5. Despite the data scatter Fig. 5 does suggest that soil characteristics play an important role in determining aerosol production. Gillette (1977) suggests that more detailed investigation is required and cautions against the use of the present data as a predictive tool.

FIELD MEASUREMENT OF AEROSOL FLUXES

A fundamental problem in identifying and evaluating the aerosol production potential of surfaces is the need for the direct monitoring of sediment loss under a wide range of atmospheric (wind speeds and directions) and surface conditions (surface moistures, salt contents, undisturbed versus disturbed). However, direct field observations using specialized monitoring equipment, (e.g. Gillette, 1977; Nickling 1978; 1983) despite their usefulness, do have several serious drawbacks:

1) they are extremely costly in terms of the instrumentation and the logistic support necessary to investigate several sites

2) field studies are very much dependent on the vagaries of the weather and as a result one often spends considerable time waiting for the right weather or surface conditions that in the end may severely limit the quality and quantity of data obtained.

3) data obtained in such studies are often extremely complex because of the lack of control on the many atmospheric and surfaces variables

involved in the wind erosion process.

The Portable Field Wind Tunnel

In order to overcome some of these serious limitations of direct soil loss monitoring under natural wind conditions a portable field wind tunnel was designed and constructed for *in situ* testing. The wind tunnel is similar in design, although considerably larger than portable wind tunnels reported by Wooding (1968) and Gillette (1978). The tunnel has a 0.75 x 1.0 x 11.0 m open floored working section constructed of fiberglass with plexiglass viewing/access windows (Fig. 6). The tunnel uses a two dimensional molded fiberglass inlet bell with a honeycomb flow straightner and a conical fiberglass diffuser. Air flow for the wind tunnel is provided by a 95 cm centrifugal fan powered by a 35 h.p. diesel engine. The fan and engine are transported and operated from the bed of a three quarter ton pick-up and connected to the main working section by 1.0 m diameter flexible hosing. The inlet bell, working sections and diffuser are transported on a 10 m flatbed trailer (Fig. 6).

The wind tunnel has been successfully used for the past two years in a detailed study evaluating the effects of tillage and cropping systems on soil loss by wind on agricultural fields. The tunnel has proven to be extremely efficient and provides a valuable alternative to other instrumentation previously used in the evaluation of soil loss by wind.

Figure 6 Mesa Agricultural Site

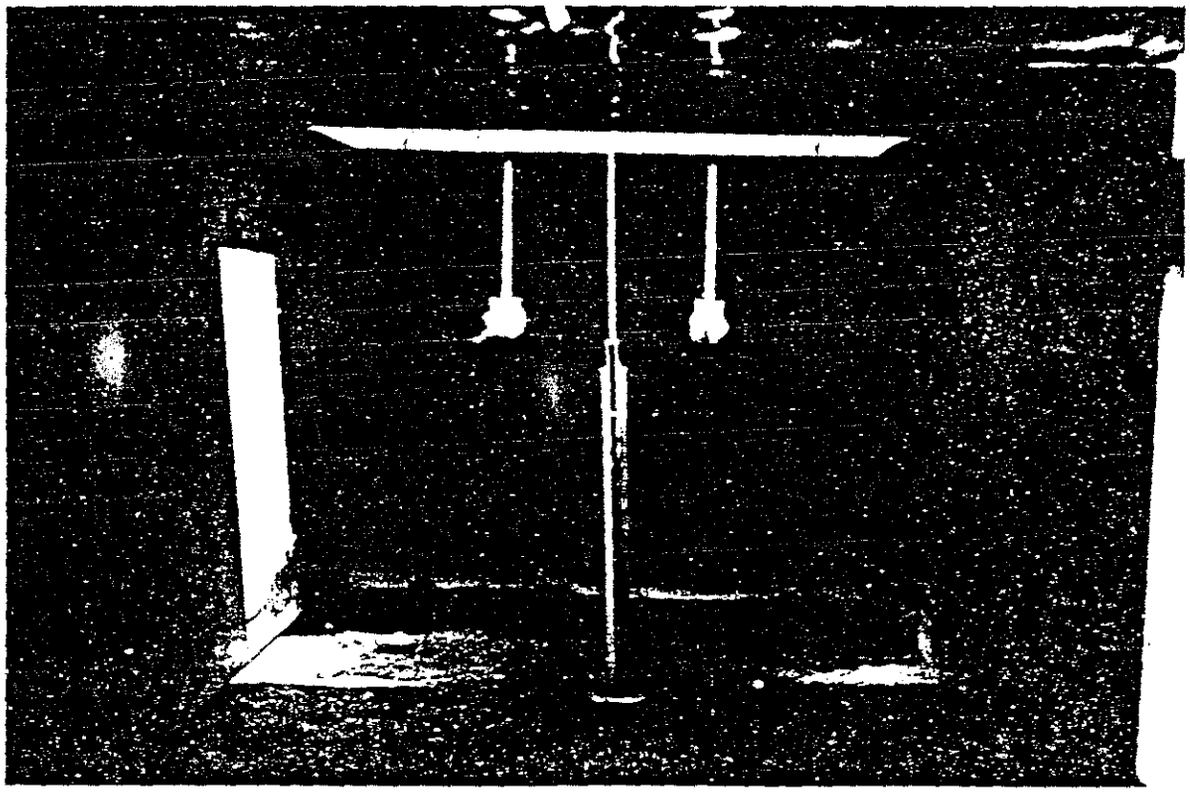

Figure 6a Suspended sediment samplers and Bagnold type trap installed in the wind tunnel.

SAMPLE SITES

A total of thirteen representative sample sites were selected for the evaluation of dust emission factors through wind tunnel testing. The types of surfaces investigated were:

	Surface Type	Location
1)	Productive agricultural land	University of Arizona Experimental Farms at a) Mesa Az. b) Maricopa Az. c) Yuma Az.
2)	Abandoned agricultural land	Casa Grande Az.
3)	Natural scrub desert	Yuma Az.
4)	Disturbed desert	a) Yuma Az. b) Algodones dune flats, Calif.
5)	Fluvial channels	a) Santa Cruz River, Tucson Az. b) Salt River, Mesa Az.
6)	Construction sites	a) Tucson Az. b) Glendale Az.
7)	Mine tailings	a) Ajo Az. b) Hayden Az.

A brief description of each sampling site follows:

Agricultural Field, Mesa Az.

The representative agricultural site for the Phoenix area was located on the University of Arizona's Experimental Farm in Mesa (Fig. 6). The field used for the tests was adjacent to Apache Blvd. and the entrance to the research station.

The soil had been tilled a few days prior to the testing by disking twice. This tillage method left a large range of clod sizes on the surface

and effectively removed any vegetation. This soil breaks up into blocky and angular clods which create a fairly rough surface. The field was previously levelled for irrigation and consequently was extremely flat. Only the clods provide any type of impedance to the wind. This site had not received any appreciable rainfall for several months and was therefore extremely dry.

Agricultural Field, Maricopa Az.

A field at the University of Arizona's Maricopa Experimental Farm was used for dust emission testing for agricultural land in the Maricopa region (Fig. 7). The test field had been laser-levelled and recently tilled using standard preparatory methods for cotton cultivation. At the time of testing the cotton crop had not been planted. The soil was extemely cloddy and was aerodynamically rougher than any other of the sites tested.

Agricultural Site, Yuma

A cultivated field on the University of Arizona's Agricultural Research Station was used as a typical agricultural field in the Yuma area (Fig. 8). The field had been laser-levelled for irrigation and was extremely flat. The surface was tilled a few days prior to testing and was very loose and friable. The size of the clods were much smaller than those of the Mesa and Manicopa sites. There was also much more disaggregated soil between the clods at this site.

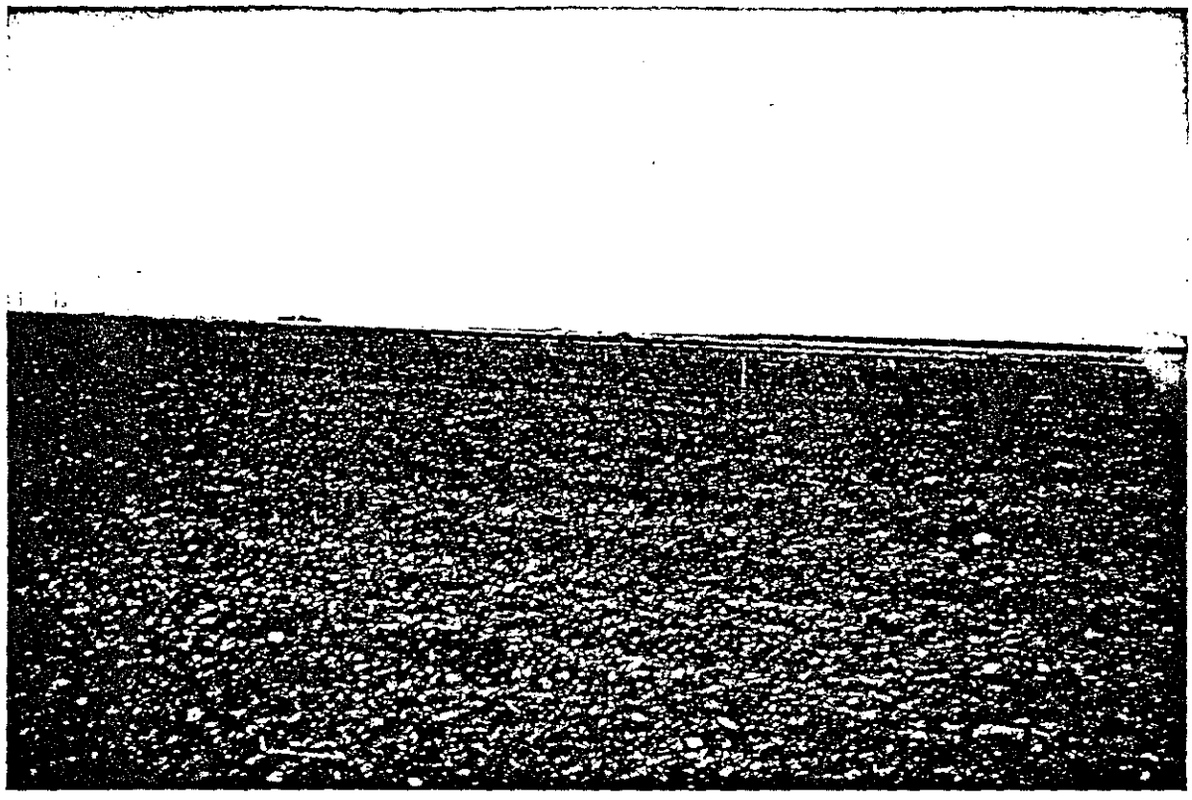

Figure 7 Maricopa agricultural site

Figure 8 Yuma agricultural site

Abandoned Agricultural Fields, Casa Grande

The Casa Grande area has large tracts of abandoned agricultural lands which are known sources of blowing dust. The test site was approximately five miles south of Interstate -10 on Toltec Rd. (Fig. 9). The field had been laser-levelled at some time and was extremely flat. There was no residual ridging apparent in the field from previous tillage operations so the surface was smooth. Vegetation was sparse with small grassy areas but the surface was generally clear. The soil in the field was easily disturbed by vehicular activity and livestock. The wind tunnel tests were done primarily on disturbed soil with no vegetation. However, one test was run on crusted soil in order to make a comparison of the effect of crusting.

Natural Desert, Yuma

An area of relatively undisturbed desert was located for testing, west of the Gila Mountains on B.L.M. land (Fig. 10). The area on which the testing took place was flat with sparse vegetation cover. The surface had a typical pebble lag deposit and the soil exposed between the pebbles was lightly crusted. The soil crust was extremely delicate and broke with the slightest pressure. Saltating particles easily broke the crust once the wind tunnel tests were initiated.

Disturbed Desert Yuma

Property within the University of Arizona's Agricultural Research

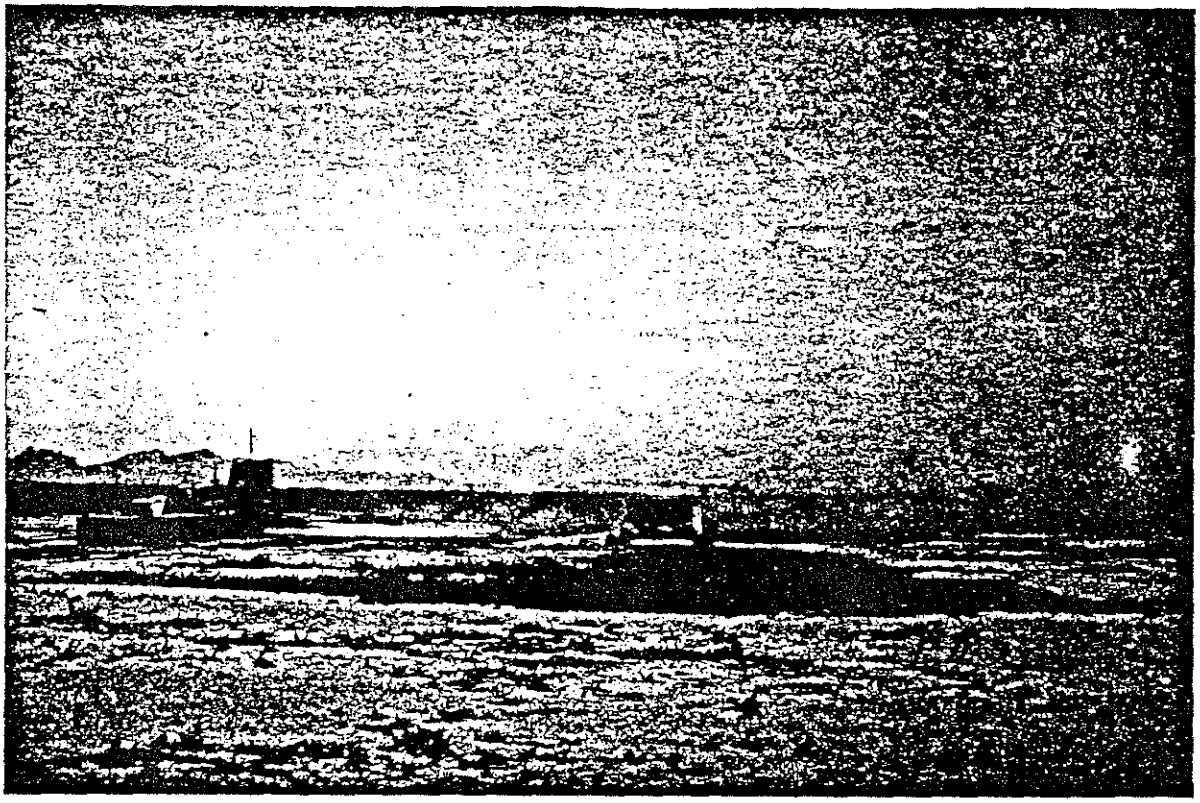

Figure 9 Abandonned agricultural field site at Casa Grande, Az.

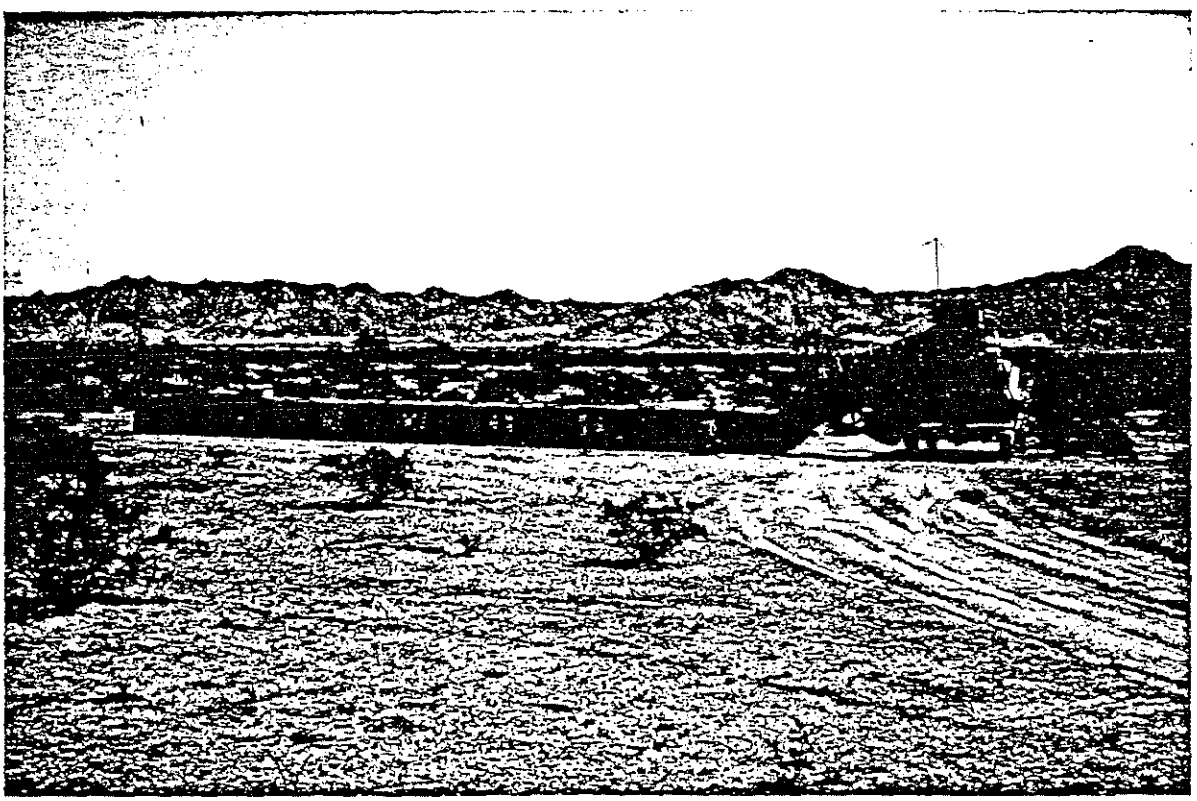

Figure 10 Scrub desert site, Yuma, Az.

Station, Yuma, was typical of a disturbed desert environment. The natural vegetation and soil had been disturbed by vehicular traffic (Fig. 11). A representative area within this environment was chosen for emission testing. The site was moderately level with some gentle slopes. The surface soil was very loose and exhibited little cohesive structure. The surface was smooth except for small clumps of grasses. The protruding bunches of grass were generally 2 - 3 cm high and 3 - 5 cm in diameter. The grass clumps occasionally grouped together in larger aggregations and reached 8 - 10 cm in height. Other typical vegetation such as creosote and sagebrush were widely scattered. The ratio of vegetation cover to exposed soil was low. In general the area was dominated by loose soil.

Algodones Dune Flats

The Algodones Dune area was suspected as being a source area for atmospheric dust. However, textural analysis of the sands indicates that the silt content is less than one percent. Surrounding the dune area proper are extensive fluvial outwash deposits which are a more likely source of dust (Fig. 12). A site was chosen on these alluvial deposits on B.L.M. land off I-10 on Sidewinder Rd. These flats are disturbed regularly by off-road vehicles which continually renews the supply of wind transportable silt size particles at the surface. The site was relatively flat with a lag deposit of small gravel size particles spread over the surface. This area contains a typical assembledge of desert plants and is sparsley vegetated.

Figure 11 Disturbed desert site, near Yuma, Az.

Figure 12 Algodones dune flats, Ca.

Salt River, Mesa

The emission tests for the Salt River were carried out in the channel approximately one quarter mile upriver from the Hayden Rd. Bridge, in Mesa (Fig. 13). At this location large silt lenses had been formed in the backwater zones during flood stages. These silt lenses are slightly undulating and are quite variable in size. The silt lens tested covered several tens of square yards. The surface was very loose with no evidence of crusting. The river channel at this location is heavily trafficked by off-road recreational vehicles which may account for the loose nature of the sediment.

Santa Cruz River, Tucson

The river channel site in Tucson was located on the Santa Cruz River off I-10 at Orangegrove Rd. (Fig. 14). The dry river bed and terraces of the Santa Cruz are regularly disturbed by off-road vehicles and the silt is readily available for transport. The area on which the wind tunnel tests were run was a terrace above the flowing section of the river. The terrace was very flat with sparsely scattered vegetation and showed evidence of vehicular disturbance. The surface was very silty and contained small gravel particles which were left as a lag deposit after the surface was exposed to erosive winds.

At the time of testing Tucson had been experiencing evening thunderstorm activity. To ensure the surface was at its lowest moisture content, testing was done in the afternoon. The rainfall events may have

Figure 13 Disturbed river channel site, Salt River, Mesa, Az.

Figure 14 Disturbed river channel site, Santa Cruz River, Tucson, Az.

had some crusting effects on the soil.

Construction Site, Tucson

The Tucson construction site test area was located on the south side of I-10, where a major new motel complex is being constructed (Fig. 15). The site had been levelled by earth moving equipment and consequently was flat and devoid of vegetation. The surface soil had been heavily pulverized as a result of heavy vehicle traffic. The fetch lengths over this one half mile square area were completely uninterupted in all directions.

The site of the wind tunnel testing was on the loose disturbed soil from which the major dust emissions can be expected. The susceptibility to wind transport of this soil has been ameliorated by watering operations and one test was run on the stabilized surface for comparison purposes. The effectiveness of watering the soil is lost if vehicles re-disturb the surface.

Construction Site, Glendale Ariz.

The construction site for the new west campus of Arizona State University was tested to determine typical emission factors for construction sites in the Phoenix area (Fig. 16). The soil at this site had been severely disturbed by earth moving equipment and levelled with laser controlled heavy equipment removing all vegetation. Exposed, uninterupted fetch lengths approach one half mile in length.

The earth moving operations have pulverized the remaining soil on the

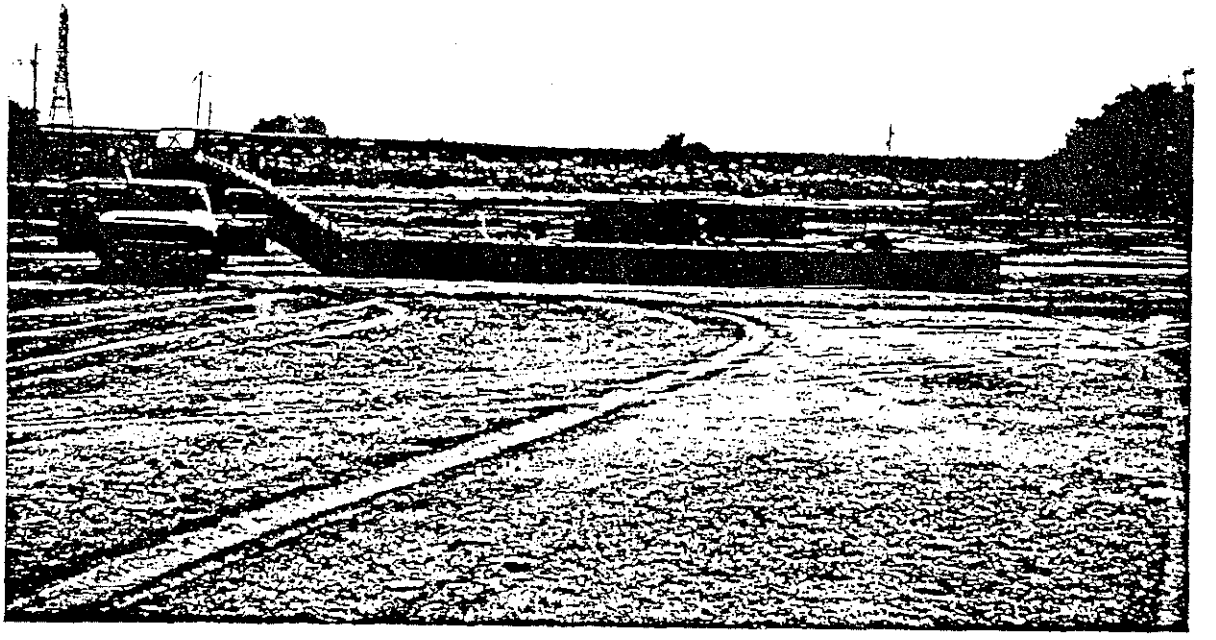

Figure 15 Construction site, Tucson, Az.

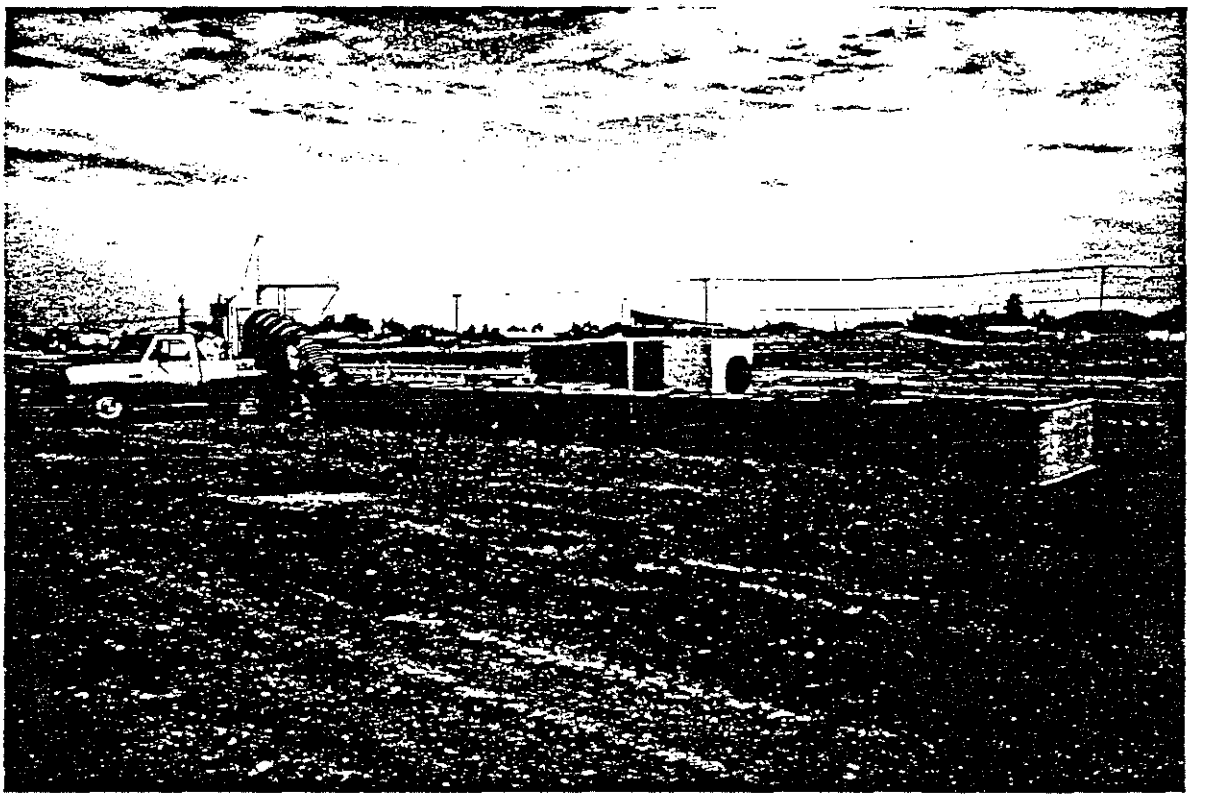

Figure 16 Construction site, Glendale, Az.

site, and the silt size particles in this soil are continually available for transport. There is also some percentage of gravel in the soil which is left behind as a lag deposit after an erosion event. Disturbance of the surface is especially prevalent where the earth-movers are operating and on the roadways. Extensive watering operations however, have succeeded in stabilizing large areas by creating a crusted surface. The watered areas reduce the potential erosion but are easily disturbed by vehicular traffic.

Mine Tailings, Ajo

The mine tailing test site in Ajo was on the property of the Phelps-Dodge Co. The tailings were produced from the copper mining operation which has now been shut down (Fig. 17). The tailing ponds are extensive in area, up to several square kilometres, extremely flat and devoid of vegetation owing to the caustic nature of the tailings.

The tailings have very little cohesive structure at the surface and with depth. There was no evidence that the surface would become armoured with non-erodible particles at any time. The tailing particles are virtually all of transportable size at naturally occurring wind velocities making this site an extremely productive particulate source.

Mine Tailings, Hayden

The Hayden tailing site was morphologically similar to the Ajo tailings but there was greater cementation of the tailings in undisturbed areas (Fig. 18). The major reason for this was the textural difference in the sediment

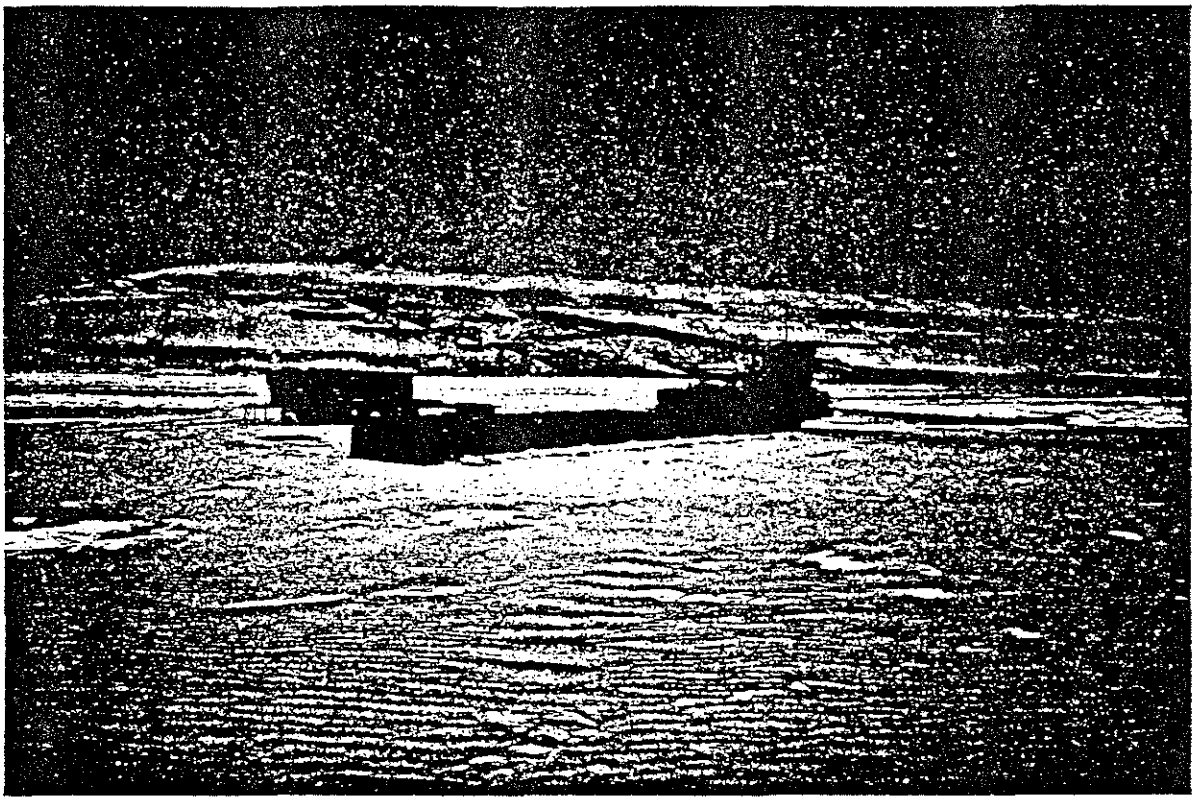

Figure 17 Mine Tailings at Ajo, Az.

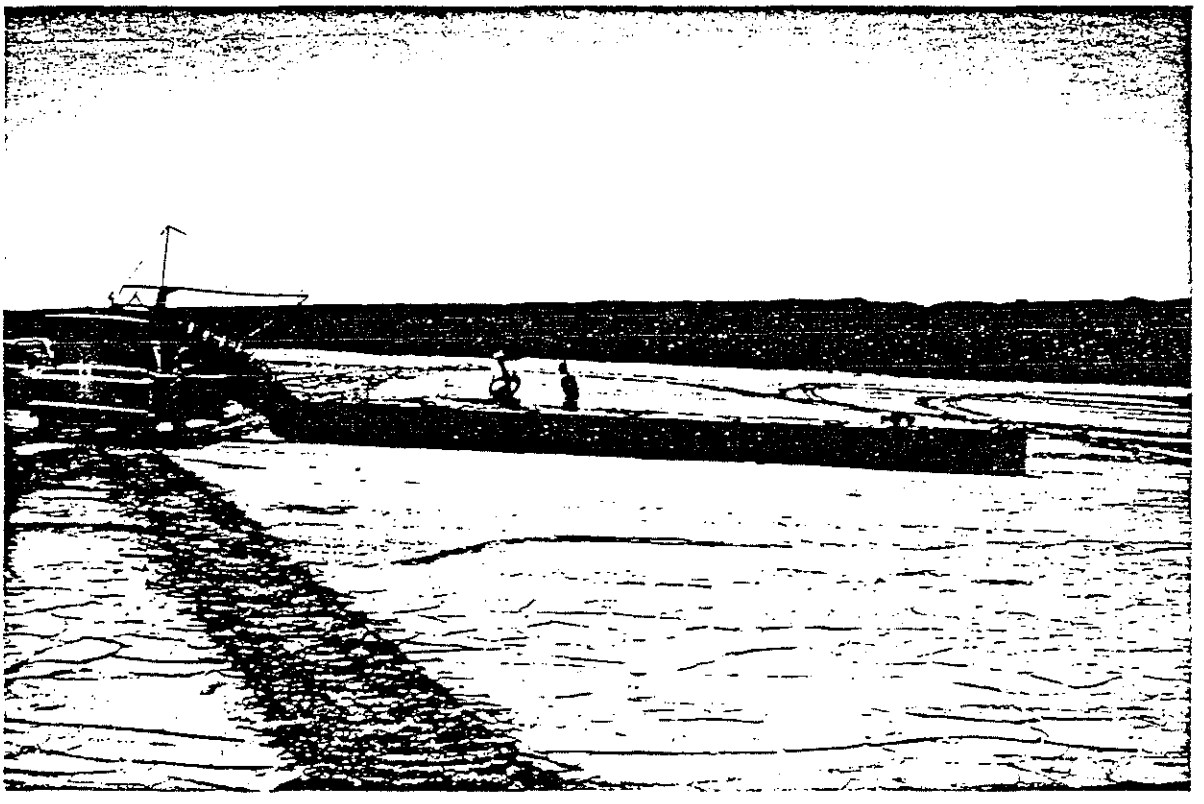

Figure 18 Mine Tailings at Hayden, Az.

between the two sites. The Hayden tailings have a much higher silt content. The higher percentage of silt creates greater cohesive forces especially if the wet tailings are left undisturbed until dry. However, there is an increased potential for increased emission levels upon disturbance because more silt is available for transport.

The wind tunnel testing was on tailings which had been disturbed by heavy vehicles and on roadways composed of tailings. To compare the difference between disturbed and undisturbed, one test run was done on undisturbed, cemented tailings and another on a roadway of tailings covered with decomposed granite, which is another by product of the mining process.

TESTING PROCEDURES

The wind tunnel was carefully placed over the test site surface. Following this the wind velocity sensors and sediment collectors were installed into the testing section. Velocity was measured with four N.P.L. type pitot tubes connected to magnehelic pressure gauges. The pitot tubes were positioned above the soil surface at heights of 5, 15, 25 and 35 cm.

Suspended sediment was collected in two streamlined isokenetic samplers mounted downwind and to either side of the pitot tube 50 cm above the surface (Fig. 6a). The samplers were connected to a high volume vacuum pump. Sediment was collected during each run by drawing air isokinetically through 3.7 cm diameter membrane filters (0.1 μm pore diameter) held in commercially available sampling cassettes within the samplers. Isokinetic flow through the 0.64 cm sample orifice was maintained during each test by means of a needle valve and flow meter which was incorporated into each

vacuum line.

To collect sediment moving in saltation and creep, a Bagnold type catcher was installed 10 cm behind the suspended sediment collectors along the centre line of the tunnel. The Bagnold catcher is 50 cm in height with a 1.0 cm wide sampling orifice (Fig. 6a).

Following installation of the instrumentation, velocity in the wind tunnel was slowly raised until movement of particles was noted by observers positioned at the plexiglass viewing windows. After the threshold test was completed a predetermined shear velocity (u_*) above threshold was established in the wind tunnel and the suspended sediment nozzle flow rate set to the centre line velocity at the instrument height. The length of the individual test was dependent on the amount of sediment transported and was longer for surfaces with lower flux rates. Duration of individual tests ranged from 10 to 30 minutes. At the completion of the test run the sediment samples were removed from the samplers and carefully stored for subsequent weighing and grain size analysis.

Typical wind velocity profiles measured during the tests are shown in Fig. 19. As can be seen, the profiles closely follow a log-linear relationship as predicted by the Prandtl equation (Eq. 1).

Since the soil surface may become depeleted of erodible grains during the test, it was necessary to move the tunnel to a new location for each sample run. Subsequent test locations were normally within 10 m of the original site with the long axis of the tunnel parallel to the initial orientation. Once the wind tunnel was repositioned the threshold determination and flux measurements were repeated. In general, five or six runs were carried out at each of the 13 selected sites. In some cases not

VELOCITY PROFILES

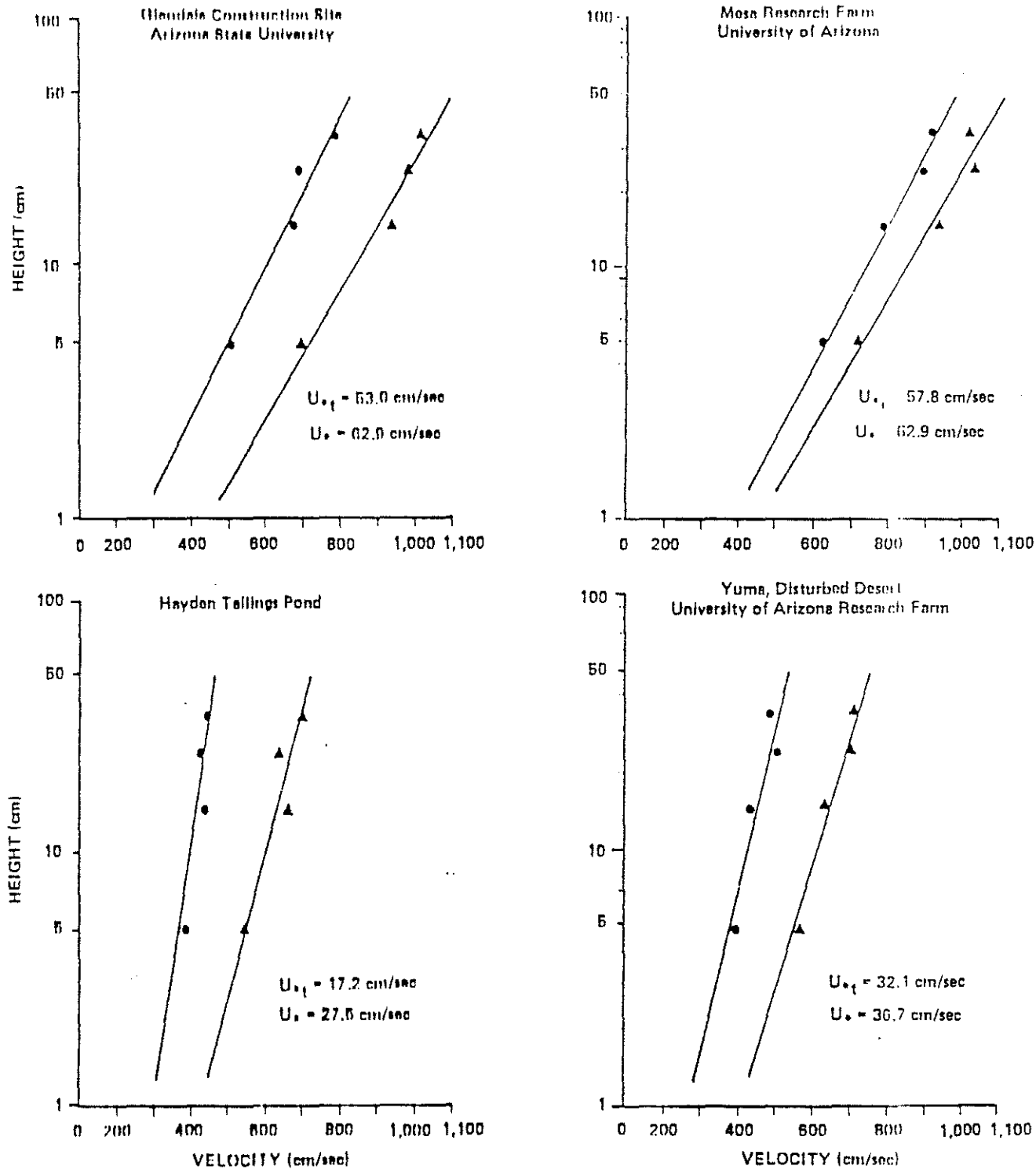

Figure 19

all runs were conducted on the same surface type. For example at Hayden: 3 tests with increasing shear velocities were carried out on the disturbed tailings, one test on the undisturbed crusted surface, one test on the disturbed tailings roadway which had been armoured with fine granite gravel in an attempt to decrease particulate emissions. The collected data and surface conditions for each test are given in Table 2.

Size analysis of the suspended sediment collected during each run was done using a Quantimet 720 image analysing computer following the method of Perrie and Peach (1973). In this technique, a small portion of an aqueous dispersion of the sample is placed on a gelatin-coated microscope slide with a pipette. The water is quickly absorbed by the gelatin, leaving the individual grains dispersed and cemented on the slide. The slide is then placed under the optical microscope of the Quantimet 720. By setting class limits the instrument can be programmed to measure the total particle area larger or smaller than any of the given limits. In using this technique the class limits are based on the diameter of a circle with an equivalent area. In practice, accuracies of better than 1 percent can be obtained when the measured area covers more than 5 percent of the viewing area (Peach and Perrie, 1974). For each of the suspended sediment samples analysed, over 2000 grains were counted on each slide. Results of the grain size analysis for the specified size classes, < 1.0, 1.0-2.5, 2.5-10.0 and > 10.0 μm are shown in Table 6.

TABLE 2

THRESHOLD DATA FOR THE TEST SITES

Location	Site	Average Threshold Shear Velocity U_{*t} (cm/sec)	Average Threshold Velocity of 10 metres U_{*10m} (cm/sec)	Roughness Length Zo (cm)	% Silt and Clay of Surface Sediments
Mesa Agricultural Site	A	56.9	1562.7	0.0331	18.6
Glendale Construction Site	B	53.0	1469.0	0.0301	24.7
Maricopa Agricultural Site	C	57.8	1382.3	0.1255	11.2
Yuma Disturbed Desert	D	32.0	811.3	0.0731	3.2
Yuma Agricultural Site	E	58.2	1658.9	0.0224	8.8
Algodones Dune Flats	F	62.5	1831.3	0.0166	15.2
Yuma Scrub Desert	G	38.6	1132.9	0.0163	17.2
Santa Cruz River, Tucson	H	18.0	517.5	0.0204	20.9
Tucson Construction Site	I	25.1	726.1	0.0181	14.3
Ajo Mine Tailings	J	22.8	664.5	0.0176	8.9
Hayden Mine Tailings	K	17.2	511.4	0.0141	27.3
Salt River, Mesa	L	21.8	668.2	0.0100	27.7
Casa Grande Abandoned Agricultural Land	M	24.6	780.2	0.0067	26.6

TEST RESULTS

Threshold Shear Velocity

Results of the threshold tests for the study sites are presented in Table 2. Threshold shear velocities for the sampled surfaces vary markedly but are similar to threshold values found by Gillette et al (1980) for a variety of undisturbed and disturbed desert sites in the Mojave Desert (Table 1). Also included in Table 2 are the associated 10m wind velocities required to initiate particle motion. The 10 m velocities were computed using the Prandtl equation (Eq. 1) and the roughness lengths found during the wind tunnel tests.

Although there is considerable overlap between the threshold values of the undisturbed and disturbed sites, the disturbed surfaces in general have considerably lower threshold wind speeds. This finding is consistent with the data of Gillette et al (1980).

The 10 m threshold velocities indicate that wind erosion could be initiated at all sites under most normally occurring natural wind conditions. However, the relatively high threshold values found at the Algodones dune flat site and the three active agricultural sites would suggest that major wind erosion events would be relatively infrequent considering the range of naturally occurring wind velocities.

Chepil (1951) and Gillette et al. (1980) have shown a general increase in threshold shear velocity with an increase in the modal size of the surface aggregate size distribution. It should be noted, however, that these relationships are relatively weak and demonstrate the inherent variability in natural sediments. Despite this known variability no clear

relationship appears to exist between modal size and U_{*t} for the 13 Arizona sites. This most likely results from the similarity of modal diameters for the sampled sites and the complicating effects of other surface parameters such as vegetation and surface crusting which are not evaluated in a simple bivariate relationship.

A significant relationship however, was found to exist between threshold shear velocity and the percentage of aggregates > 0.84 m (20 mesh) (See Fig. 20). This best fit least squares relationship is

$$U_{*t} = 20.09\ (\%\ \text{aggregates} > 0.84\ \text{mm})^{0.202} \quad \ldots 14$$

$$r = 0.58$$

Larger particles at the surface effect the threshold shear velocity in at least two ways. First, larger grains or aggregates which may be too large to be transported at a given velocity protrude above the surface and absorb a large proportion of the shearing stress exerted by the wind. This effect is noticeable even when the concentration of these non-erodible units is relatively small (Chepil, 1951). Second, larger stationary particles tend to shield smaller, more easily entrained particles from the wind shear. Consequently as the concentration of non-erodible unit increases the threshold shear velocity also increases.

Chepil (1951, 1955) has shown a similar relationship between soil erodibility and percentage of aggregates greater than 0.84 mm. Although the relationship shown in Fig. 20 is relatively weak it does provide an alternative to the Bagnold equation (Eq. 6) for threshold determination of aggregated natural desert soils. Despite the fact that the Bagnold equation

THRESHOLD SHEAR VELOCITY
VERSUS % AGGREGATE > 0.84 MM

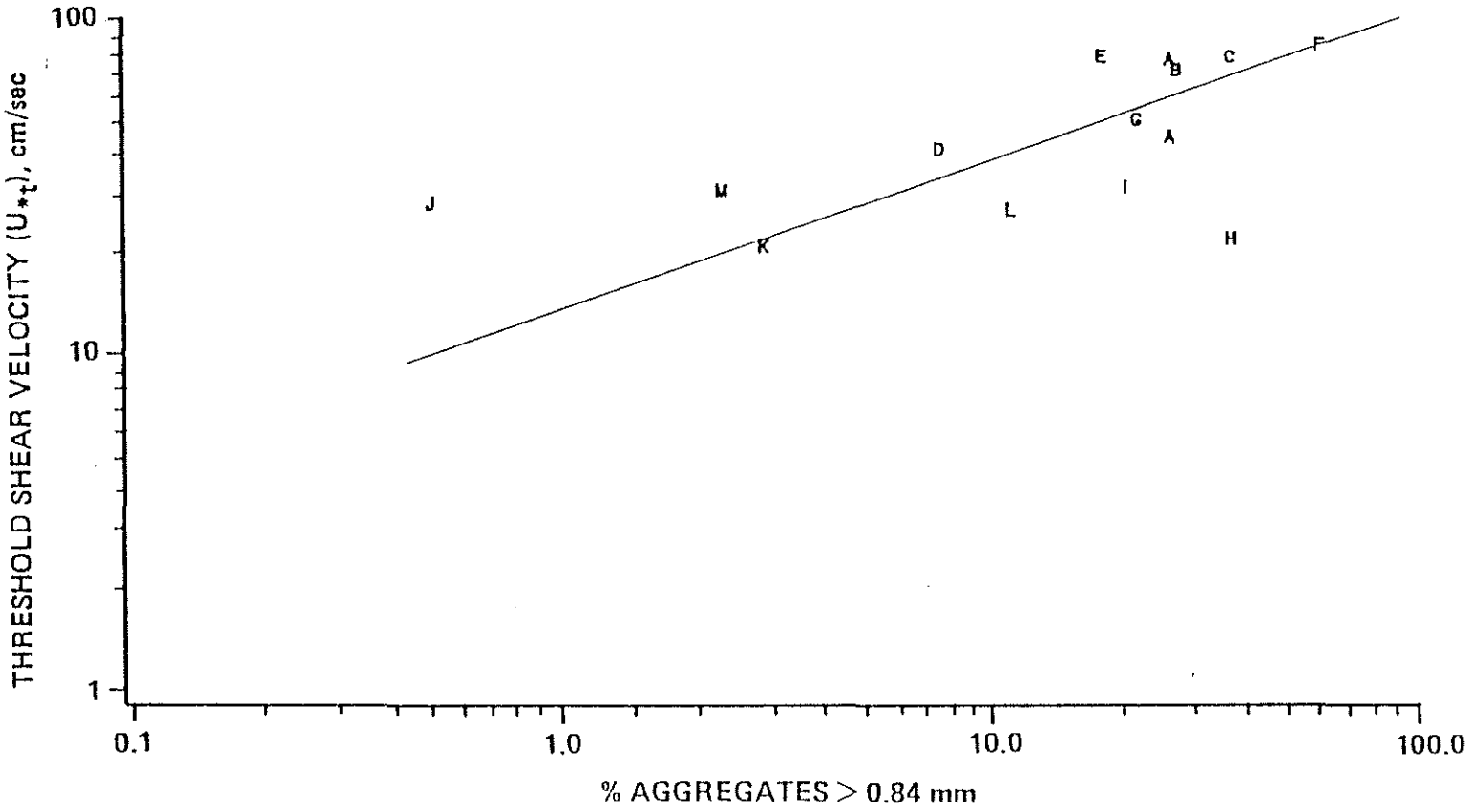

Figure 20

is frequently used by investigators to determine threshold velocities of natural soils, it is often used inappropriately. As discussed previously, the Bagnold equation in the strictest sense, only holds true for relatively well sorted dispersed grains greater than approximately 0.1 mm in diameter. The potential error in using the Bagnold equation for aggregated soils with high silt content is clearly shown in Fig. 21. In this figure measured U_* values for the 13 sampled sites are plotted against U_* values calculated from the Bagnold equation using the mean grain size of the surface sediments. In general the Bagnold equation tends to over-estimate the measured shear velocity but with no consistent pattern.

Gillette et al. (1980, 1982) have also addressed the question of threshold velocity of natural soils in a detailed study of 37 sites located primarily in the Mojave desert. These authors present a series of empirical relationships derived from field wind tunnel tests relating threshold shear velocity (U_{*t}) and various textural parameters. A summary of their results are given in Table 3. These formulae, which are derived from a wide range of soil types, can be used in conjunction with the formula derived from the Arizona data for the prediction of threshold shear velocity.

Vertical Aerosol Fluxes

The mean suspended sediment concentration at the sampling height (50 cm) in the wind tunnel during each test was calculated by:

$$n = \frac{\bar{W}}{FR.t} \qquad \ldots 15$$

COMPARISON OF MEASURED AND CALCULATED
THRESHOLD SHEAR VELOCITIES

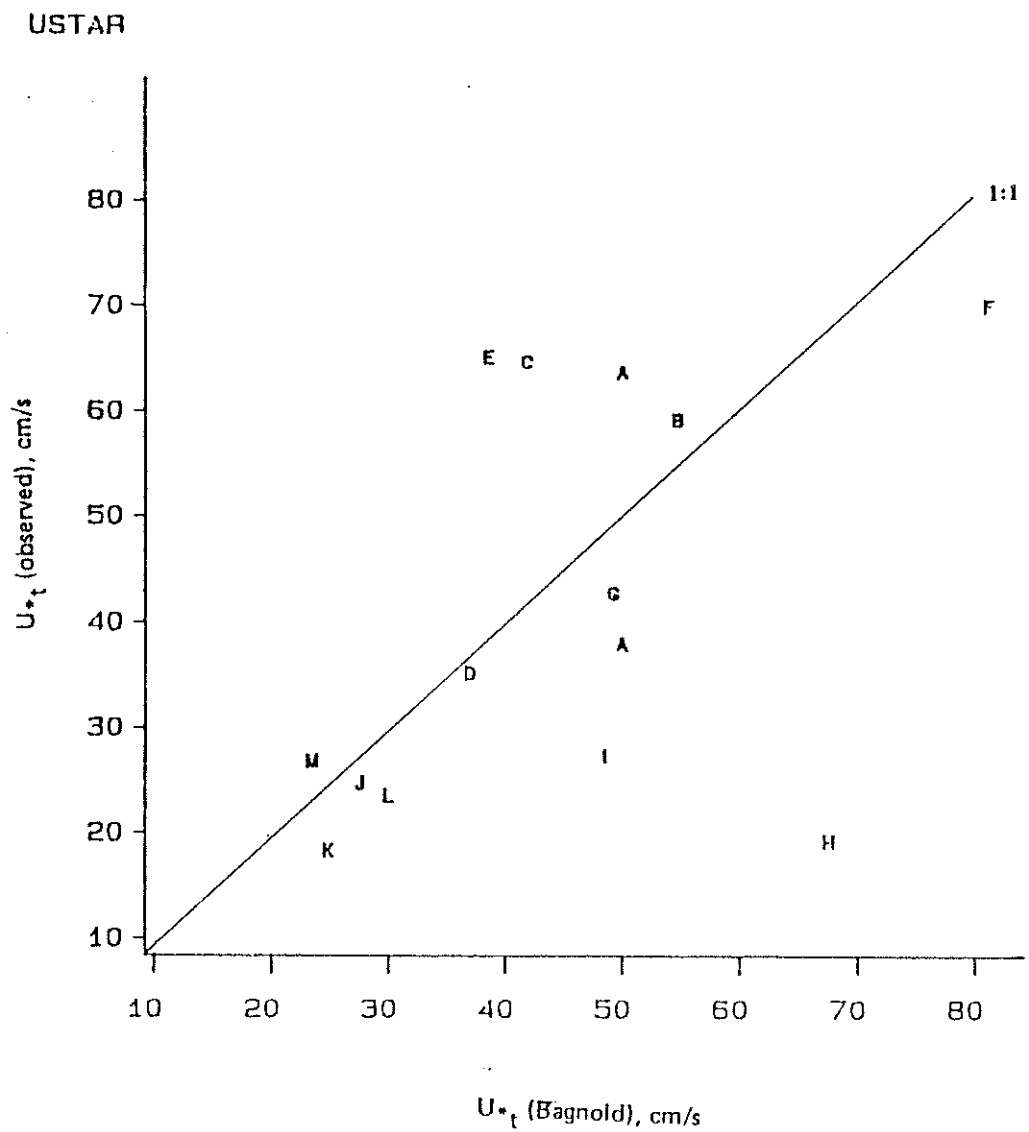

Figure 21

TABLE 3

THRESHOLD SHEAR VELOCITIES FOR VARIOUS SOIL TYPES

Undisturbed Soils	
Clay content > 20%	$U_{*t} > 200$ cm/s
Clay content < 20%	$U_{*t} = 390 - 3.3$ (% sand)
	or
	$U_{*t} = 53 + 5.1$ (% silt)
Disturbed Soils	
Sand content > 90%	$20 < U_{*t} < 60$ cm/s (variable)
Clay content < 10%	$U_{*t} = 14.5 + 0.0071$ (Mode) $+ 1.59$ (% colloidal clay)
Undisturbed and Disturbed	
Clay content < 20%	$U_{*t} = 64 + 0.0055$ (Mode)

N.B. Mode (μm) is the most frequently occurring aggregate size in the dry aggregate size distribution of the soil.

after Gillette et al (1980).

where n is the mean concentration (g/m^3)g, FR (m^3/sec) is the flow rate through the sampler nozzle and t (sec) is the sampling time.

Knowing the mean point concentration at the 50 cm height, the vertical aerosol flux during each test was computed using the equations derived by Shinn et al. (1976) discussed above (Eq. 13). In the calculations it is assumed that the gradient of dust concentration with height follows a power law with an exponent of -0.3. The mean vertical aerosol fluxes (F, g/cm^2.sec) measured at the thirteen selected sites are given in Table 4. The measured fluxes range from 1.0×10^{-9} to 6.5×10^{-7} g/cm^2 sec and show a wide inter-site variability. Shear velocities associated with the vertical fluxes range from 17.7 to 80.1 cm/sec.

The relationship between the vertical flux and shear velocity for all sites is shown in Fig. 22. As can be seen, there is a general increase in vertical flux with increasing shear velocity. Although the overall relationship is somewhat weak, it can be described by the following least squares regression formula which is significant at 99% confidence level:

$$F = 2.33 \times 10^{-11} U_*^{1.889} \qquad \ldots 16$$

$$r = 0.42 \qquad n = 67$$

It is noteworthy that the data shown in Fig. 22 compares very favourably with that presented by Gillette (1977) (Fig. 4 in this report) in terms of both the range of vertical fluxes observed and the degree of data scatter. Gillette's data were collected in West Texas during a four year period over 9 agricultural fields with varying textural characteristics. The great degree of data scatter in Fig. 21 most likely results from widely

Table 4

Aerosol and Surface Soil Flux Data

SITE		SHEAR VELOCITY U* (CM/S)	VERTICAL AEROSOL FLUX F (G/CM2 S)	HORIZONTAL SOIL MOVEMENT Q (G/CM S)	HORIZONTAL SOIL FLUX F (G/CM2 S)	AEROSOL/SOIL FLUX RATIO (F/Q')
Mesa	A	62.9	6.80E-09	0.0545	0.0011	6.24E-06
Agricultural	A	43.7	8.70E-09	0.0657	0.0013	6.62E-06
	A	43.4	4.30E-09	0.0191	0.0004	1.13E-05
	A	50.3	4.80E-09	0.0133	0.0003	1.80E-05
	A	53.4	1.17E-08	0.0191	0.0004	3.06E-05
	A	55.5	7.30E-09	0.0331	0.0007	1.10E-05
Glendale	B	22.1	1.20E-09	0.0514	0.0010	1.17E-06
Construction	B	36.7	3.70E-09	0.0588	0.0012	3.15E-06
	B	49.4	8.13E-08	0.0695	0.0014	5.85E-05
	B	62.6	1.18E-07	0.1655	0.0033	3.57E-05
	B	39.1	7.83E-08	0.0365	0.0007	1.07E-04
Maricopa	C	58.9	1.07E-08	0.0170	0.0003	3.15E-05
Agricultural	C	66.1	2.94E-08	0.0284	0.0006	5.18E-05
	C	41.1	1.88E-08	0.0318	0.0006	2.96E-05
	C	80.1	3.37E-08	0.0234	0.0005	7.20E-05
	C	72.3	2.60E-09	0.0036	0.0001	3.61E-05
Yuma,	D	27.5	2.03E-08	0.0983	0.0020	1.03E-05
Disturbed	D	38.3	4.79E-08	0.4247	0.0085	5.64E-06
Desert	D	59.6	8.04E-08	1.0408	0.0208	3.86E-06
	D	36.6	9.21E-08	0.3324	0.0066	1.39E-05
	D	55.9	2.04E-07	0.4015	0.0080	2.54E-05
Yuma	E	29.6	2.01E-08	0.4819	0.0096	2.09E-06
Agricultural	E	31.9	2.94E-08	0.0245	0.0005	6.00E-05
	E	34.6	5.11E-08	0.0350	0.0007	7.30E-05
	E	57.0	7.69E-08	0.0536	0.0011	7.17E-05
	E	51.7	6.66E-08	0.1246	0.0025	2.67E-05
Algondones	F	26.9	1.69E-08	0.0552	0.0011	1.53E-05
Dune Flats	F	34.3	4.90E-09	0.0793	0.0016	3.09E-06
	F	50.4	1.89E-08	0.0381	0.0008	2.48E-05
	F	49.7	3.38E-08	0.0587	0.0012	2.88E-05
	F	48.7	4.70E-09	0.0957	0.0019	2.46E-06
	F	40.4	3.07E-08	0.0424	0.0008	3.62E-05
Yuma,	G	50.5	3.68E-07	0.0597	0.0012	3.09E-04
Scrub Desert	G	40.4	5.40E-08	0.2423	0.0048	1.11E-05
	G	41.3	4.35E-08	0.0916	0.0018	2.37E-05
	G	46.7	1.76E-08	0.0797	0.0016	1.10E-05
	G	21.4	5.10E-09	0.0950	0.0019	2.68E-06
Santa Cruz	H	30.8	6.40E-08	0.1212	0.0024	2.64E-05
River, Tucson	H	41.7	3.08E-07	0.1338	0.0027	1.15E-04
	H	34.5	4.35E-08	0.4459	0.0089	4.88E-06
	H	18.9	6.00E-10	0.3549	0.0071	8.45E-08
	H	35.1	5.65E-08	0.1186	0.0024	2.38E-05
	H	18.5	1.60E-09	0.5516	0.0110	1.45E-07
Tucson	I	30.9	1.03E-08	0.0513	0.0010	1.00E-05
Construction	I	30.4	4.57E-08	0.1325	0.0026	1.72E-05
	I	50.2	6.52E-07	0.5730	0.0115	5.69E-05
	I	49.1	2.44E-08	2.4809	0.0496	4.92E-07
Ajo,	J	26.8	1.12E-08	0.0952	0.0019	5.88E-06
Mine tailings	J	31.2	2.44E-08	0.0922	0.0018	1.32E-05
	J	25.9	4.87E-08	0.2208	0.0044	1.10E-05
	J	35.0	6.11E-08	0.4330	0.0087	7.06E-06
	J	51.4	1.92E-07	0.9362	0.0187	1.02E-05
Hayden,	K	33.2	1.61E-08	2.2699	0.0454	3.55E-07
Mine tailings	K	24.6	2.13E-08	0.0527	0.0011	2.02E-05
	K	27.5	5.69E-08	0.0427	0.0009	6.66E-05
	K	41.7	1.29E-07	0.3136	0.0063	2.06E-05
	K	34.6	3.00E-09	0.5137	0.0103	2.92E-07
	K	41.7	9.91E-08	0.0380	0.0008	1.30E-04
Salt River,	L	17.7	4.00E-10	0.3217	0.0064	6.22E-08
Mesa	L	22.2	1.05E-08	0.0535	0.0011	9.81E-06
	L	41.7	6.17E-08	0.2764	0.0055	1.12E-05
	L	34.2	4.73E-08	1.3168	0.0263	1.80E-06
	L	29.6	4.49E-08	0.7904	0.0158	2.84E-06
Casa Grande	M	33.0	2.90E-09	0.4753	0.0095	3.05E-07
Abandoned	M	36.7	1.82E-08	0.0416	0.0008	2.19E-05
Agricultural	M	22.0	1.00E-09	0.0712	0.0014	7.02E-07
Land	M	35.5	4.77E-08	0.0420	0.0008	5.68E-05
	M	34.5	7.89E-08	0.3763	0.0075	1.05E-05

AEROSOL EMISSION FACTORS

ALL SITES CONSIDERED

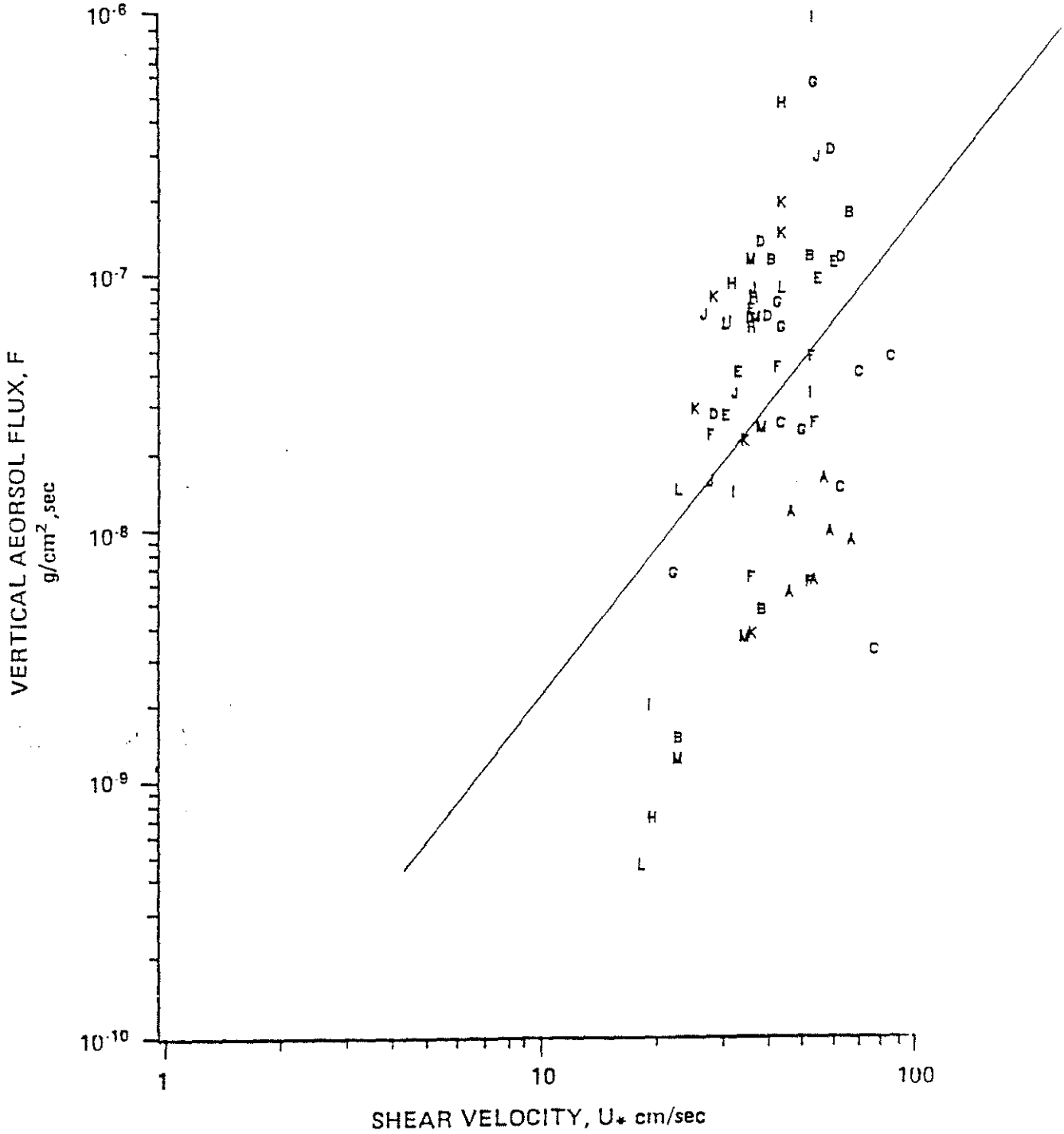

Figure 22

different textural and surface characteristics found at the sample sites. This is indicated in Figs. 23, 24, and 25 where the data have been partitioned on the basis of the percentage of silt and clay measured in the surface sediments.

Fig. 23 shows the vertical flux vs U_* for soils having a combined silt and clay content > 25%. For these silty loams a relatively high correlation exists between increasing vertical flux and U_*. The relationship is described by the least squares regression equation.

$$F = 6.12 \times 10^{-15} U_*^{4.271} \qquad \ldots 17$$

$$r = 0.75 \qquad n = 20$$

A rather weak relationship also exists between F and U_* for soils with a combined silt and clay content of 15-25% (Fig. 24). This relationship can be described by

$$F = 2.38 \times 10^{-11} U_*^{1.763} \qquad \ldots 18$$

$$r = 0.40 \qquad n = 21$$

The variation of vertical flux with increasing U_* for the sandy soils (silt and clay < 15%) is shown in Fig. 25. The very poor relationship which is evident on this plot primarily results from the inclusion of the Maricopa agricultural site data. This site, although similar in sand content to the other four sites was considerably different in terms of surface roughness characteristics. The field on which tests were carried out had been very recently ploughed and was characterized by well defined ridges 15-20 cm in height. In addition, the surface was covered with very large clods 8-10 cm

AEROSOL EMISSION FACTORS

GROUPED BY SOIL TEXTURE
SILT AND CLAY > 25%, SITES: B, K, L, M

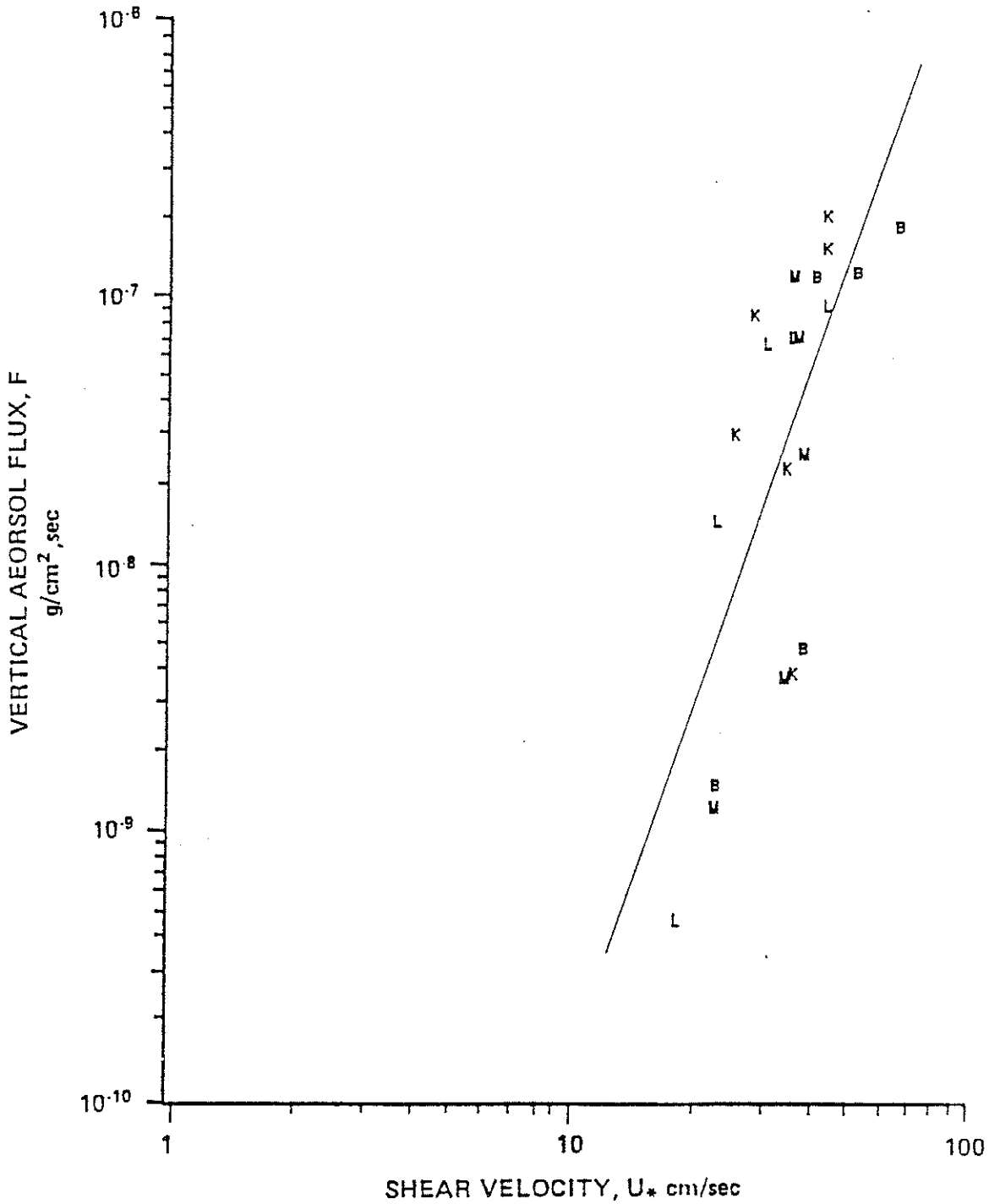

Figure 23

AEROSOL EMISSION FACTORS

GROUPED BY SOIL TEXTURE
SILT AND CLAY 15-25%, SITES: A, F, G, H

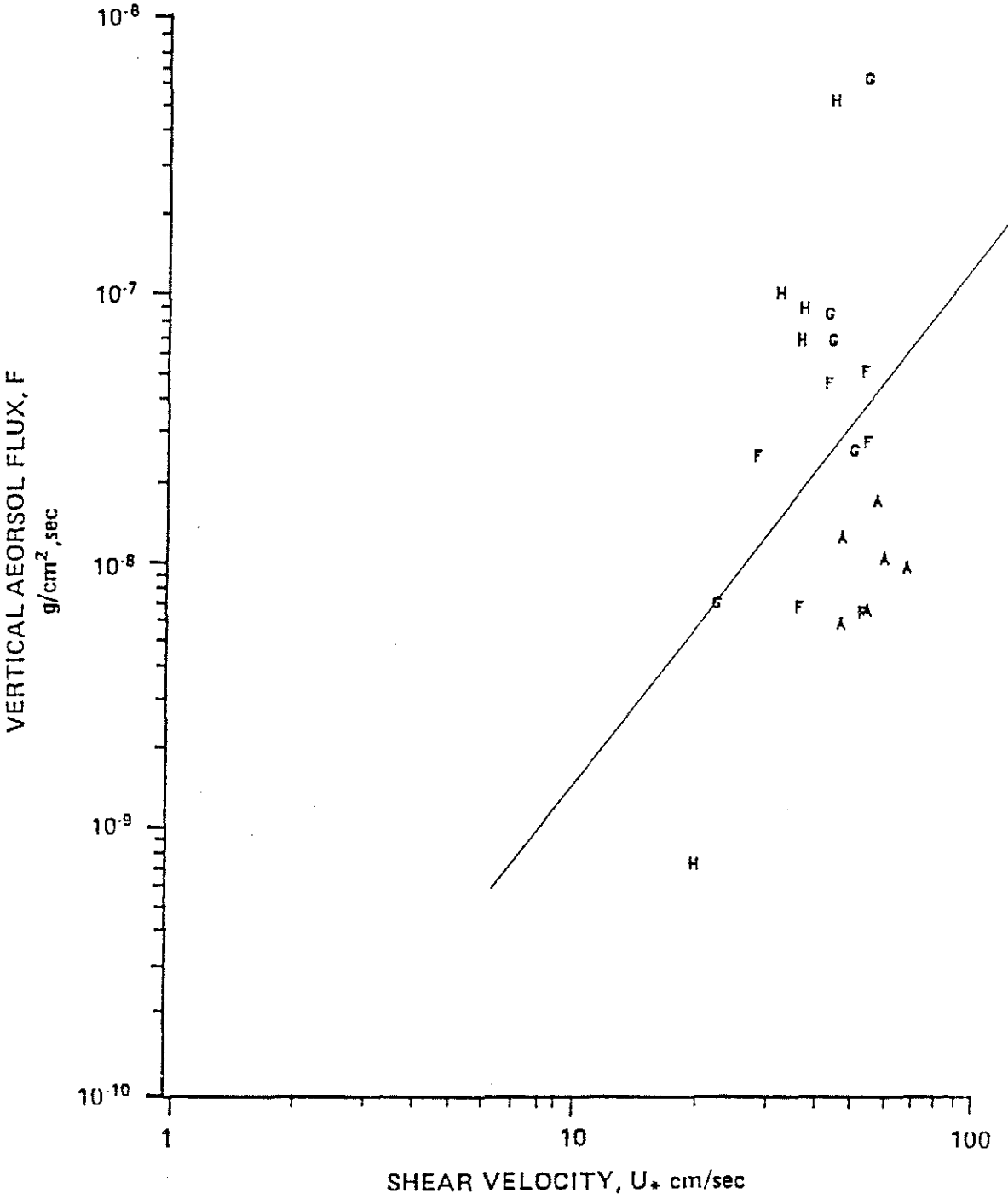

Figure 24

AEROSOL EMISSION FACTORS

GROUPED BY SOIL TEXTURE
SILT AND CLAY < 15%, SITES: C, D, E, I, J

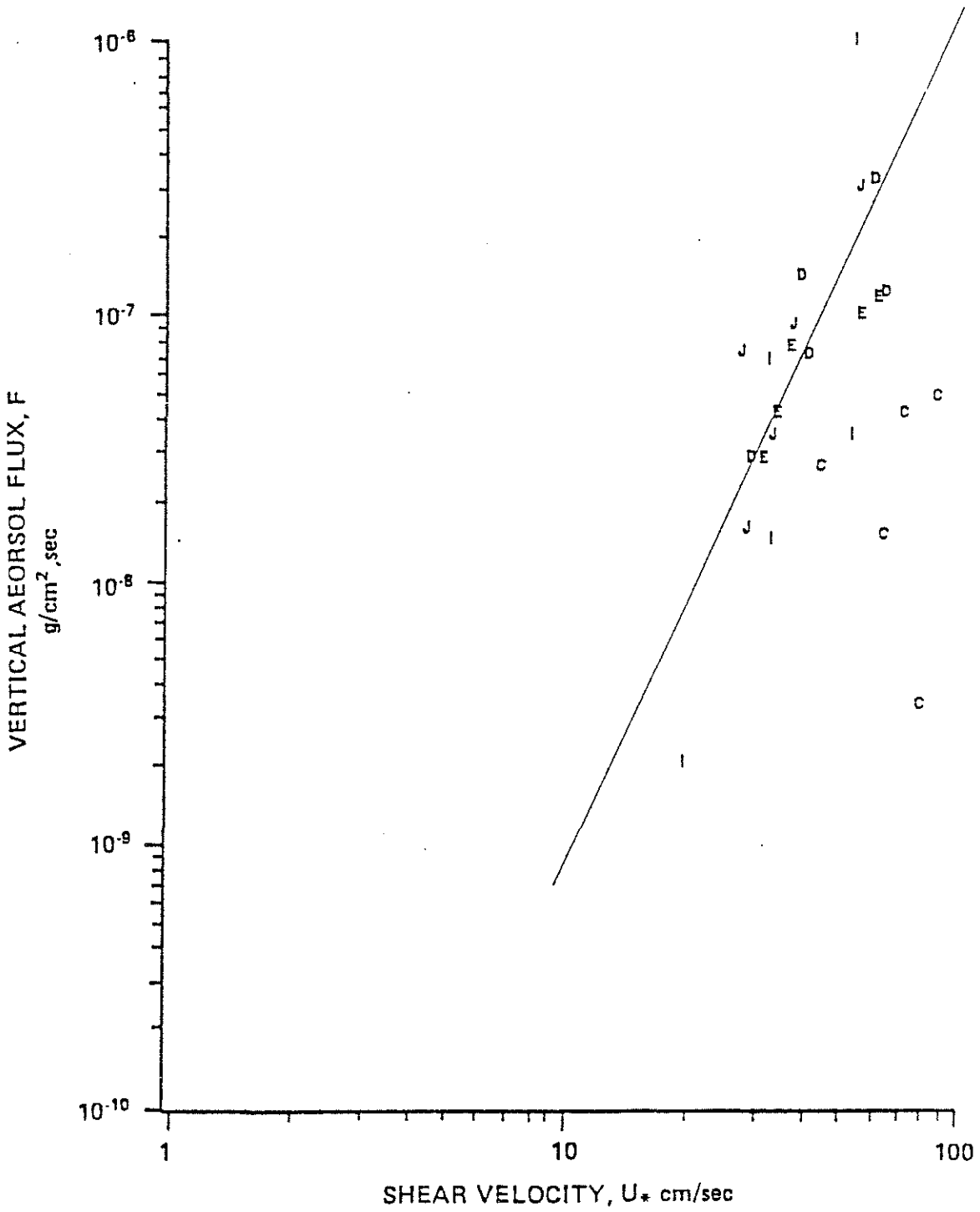

Figure 25

in diameter which most likely resulted from ploughing under somewhat moist conditions. These large relatively weak clods were not broken down by abrasion during the wind tunnel tests, and thus acted as large non-erodible roughness elements which tend to protect the finer soil fractions from deflation (Chepil and Woodruff, 1963). This results in a much less rapid increase in vertical flux with increasing shear velocity than was observed at the other four sites.

If the Maricopa data are omitted from the regression (Site C) the F vs U_* relationship for the sandy soils can be described by

$$F = 7.79 \times 10^{-13}\ U_*^{3.027} \qquad \ldots 19$$

$$r = 0.77 \qquad n = 19$$

In comparison to the above results, Gillette (1977) found a fairly uniform trend of increasing vertical particle flux with increasing shear velocity for sites with sandy soils (See Fig. 4). He attributes this relatively good relationship to the uniformity of the dry aggregate structure of the soils investigated in his study. In contrast, the vertical flux vs shear velocity for the loamy soils showed great variability which was attributed to the widely different dry aggregate structures of these soils. This argument is similar to that used to account for the lower fluxes found at the Maricopa agricultural site in the present study.

Since textural data may not be readily available when estimating emission factors for various surfaces an attempt was made to partition the data on the basis of surface morphology and/or type of activity carried out.

Despite the limited data, five classes were established:

1) Natural and disturbed desert sites
2) Sites developed or modified by fluvial processes
3) Construction sites
4) Mine tailings
5) Agriculture sites

The vertical aerosol flux curves for above classes are shown in Fig. 26 to 30. Significant regressions were derived for all classes except agricultural sites. In general, the regressions are typified by relatively high correlation coefficients and may prove useful for estimating emission rates from surfaces when textural data are lacking. A great deal of caution must be exercised, however, since the criteria on which the classes were based is somewhat arbitrary. In most instances it would be advisable to estimate emission rates from the textural relationships.

The regression relationships derived for the morphological/surface activity classes are:

1) Natural and disturbed desert

$$F = 7.99 \times 10^{-13}\ U_*^{2.99} \qquad \ldots 20$$

$$r = 0.76 \qquad n = 9$$

2) Fluvial sites

$$F = 1.59 \times 10^{-13}\ U_*^{3.32} \qquad \ldots 21$$

$$4 = 0.61 \qquad n = 15$$

AEROSOL EMISSION FACTORS

GROUPED BY SURFACE MORPHOLOGY
NATURAL AND DISTURBED DESERT SITES: D, G

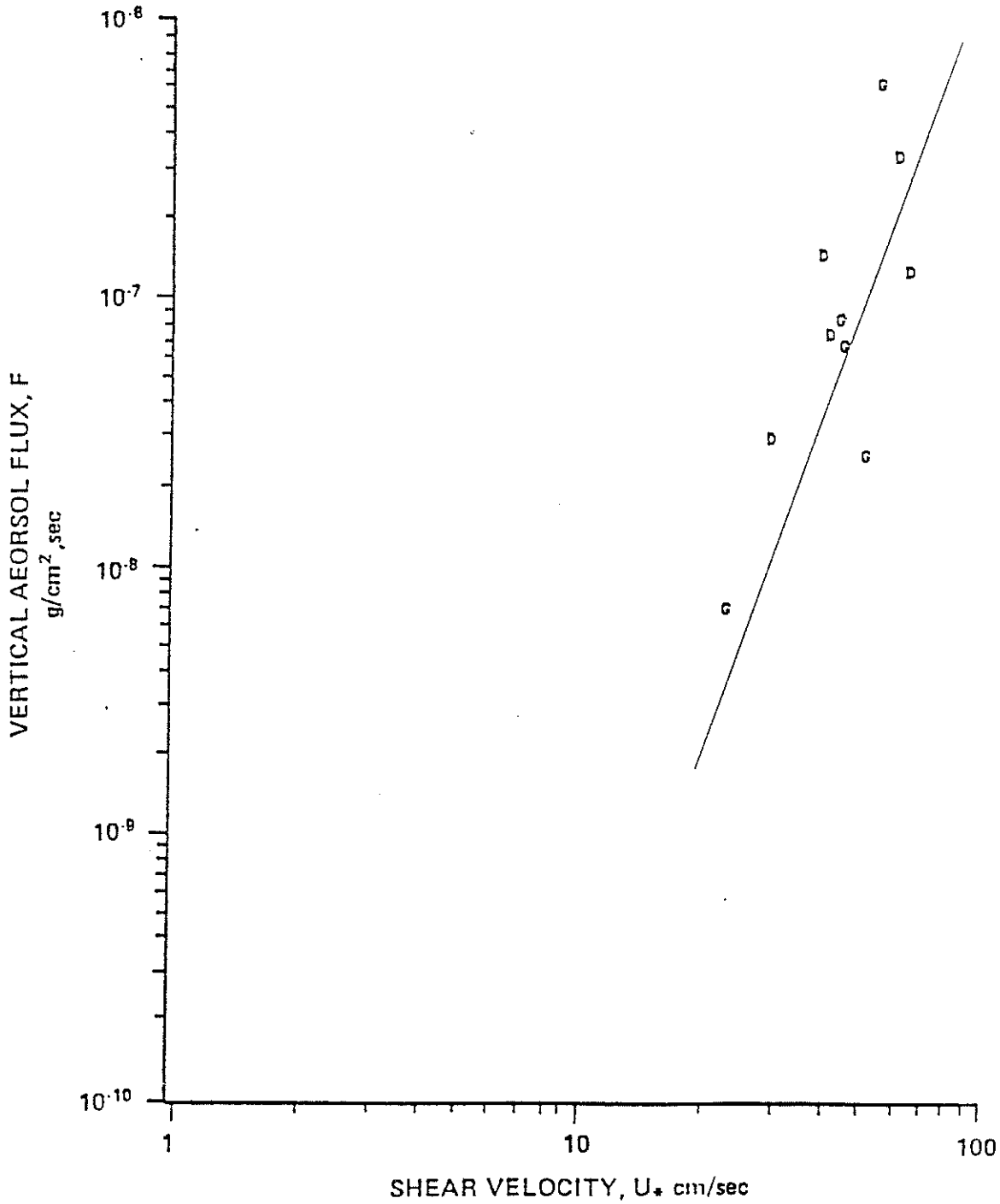

Figure 26

AEROSOL EMISSION FACTORS

GROUPED BY SURFACE MORPHOLOGY
FLUVIAL SITES: F, H, L

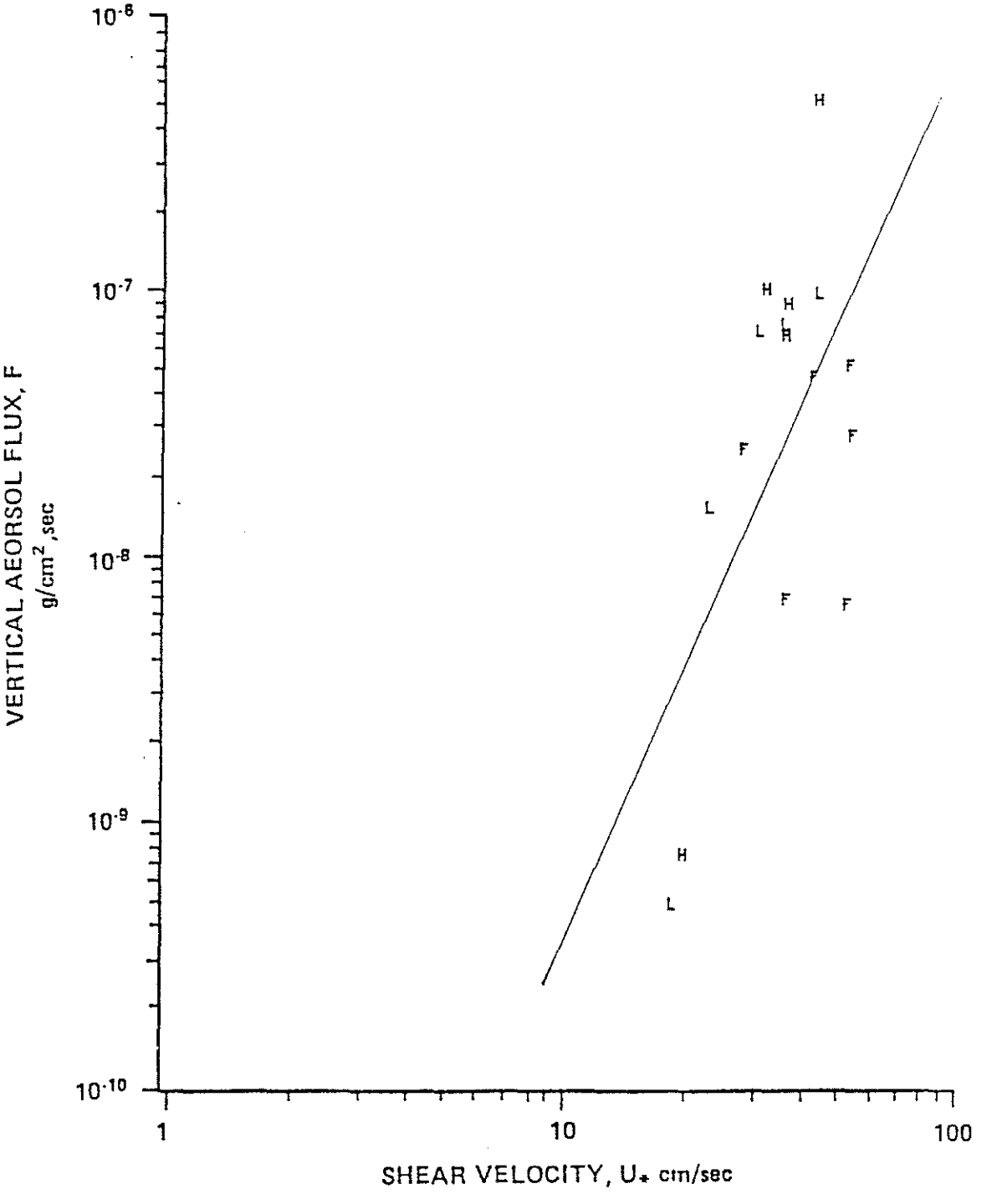

Figure 27

AEROSOL EMISSION FACTORS

GROUPED BY SURFACE MORPHOLOGY
CONSTRUCTION SITES: B, I

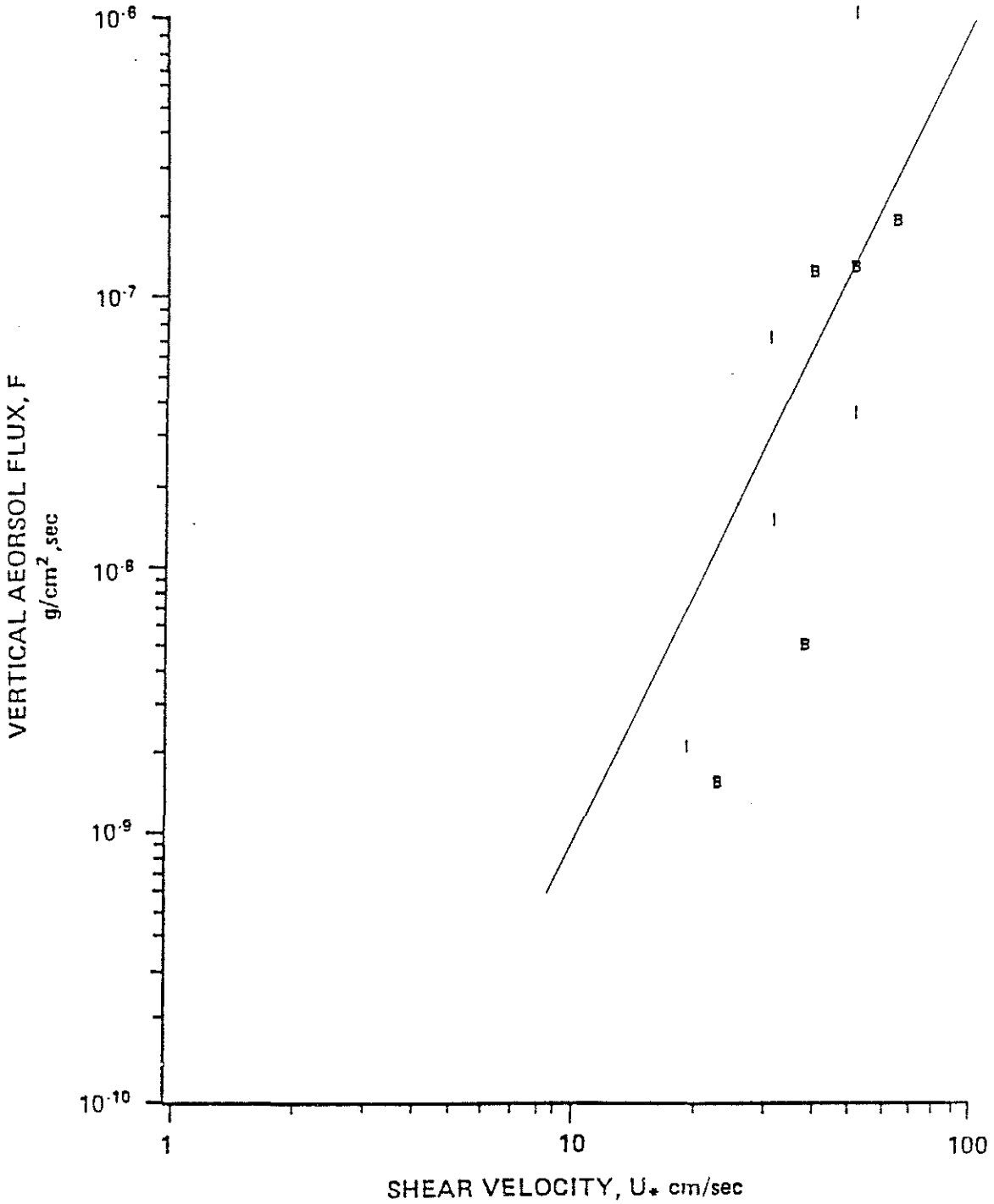

Figure 28

AEROSOL EMISSION FACTORS

GROUPED BY SURFACE MORPHOLOGY
TAILING POND SITES: J, K

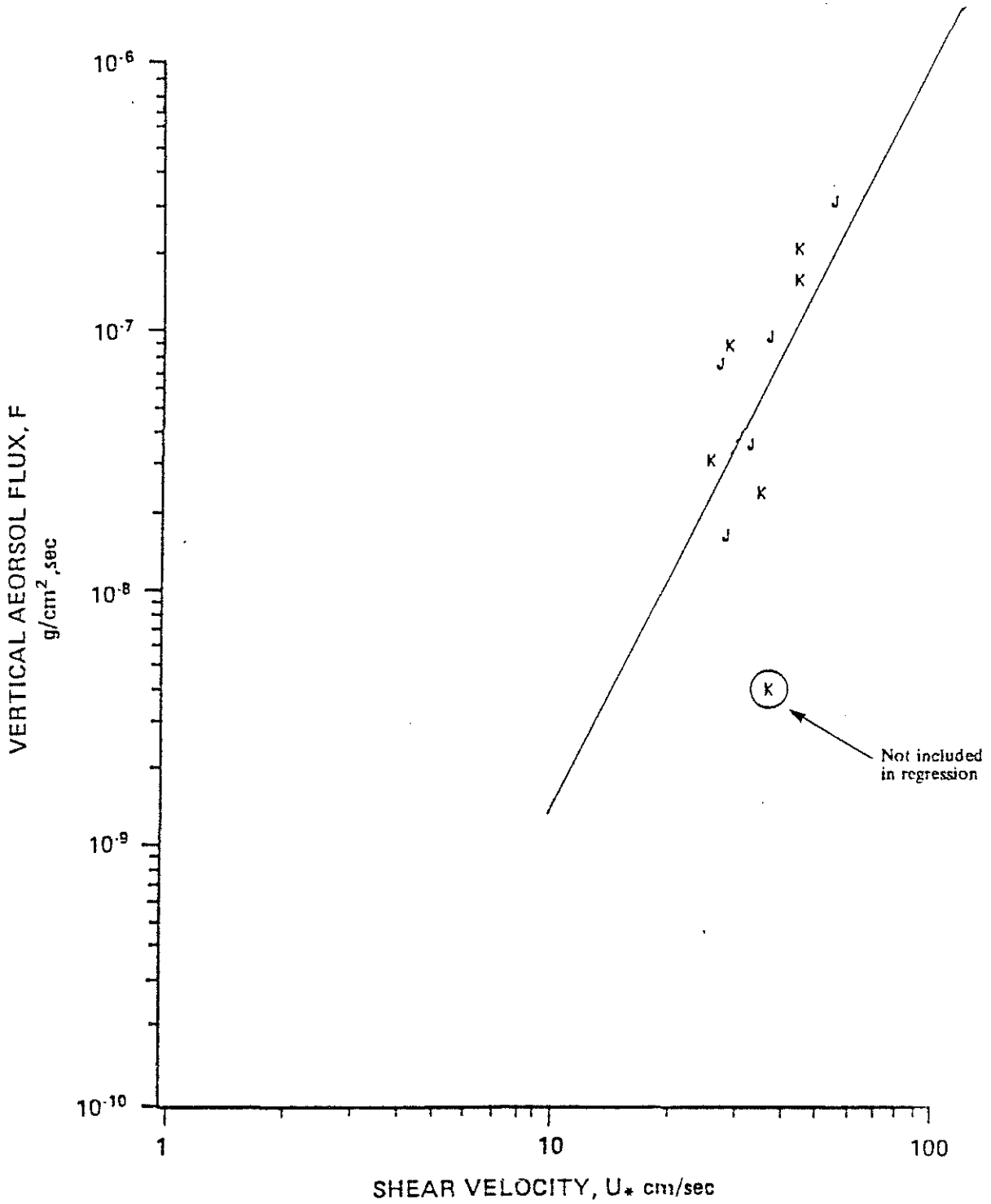

Figure 29

AEROSOL EMISSION FACTORS

GROUPED BY SURFACE MORPHOLOGY
AGRICULTURAL SITES: A, C, E, M

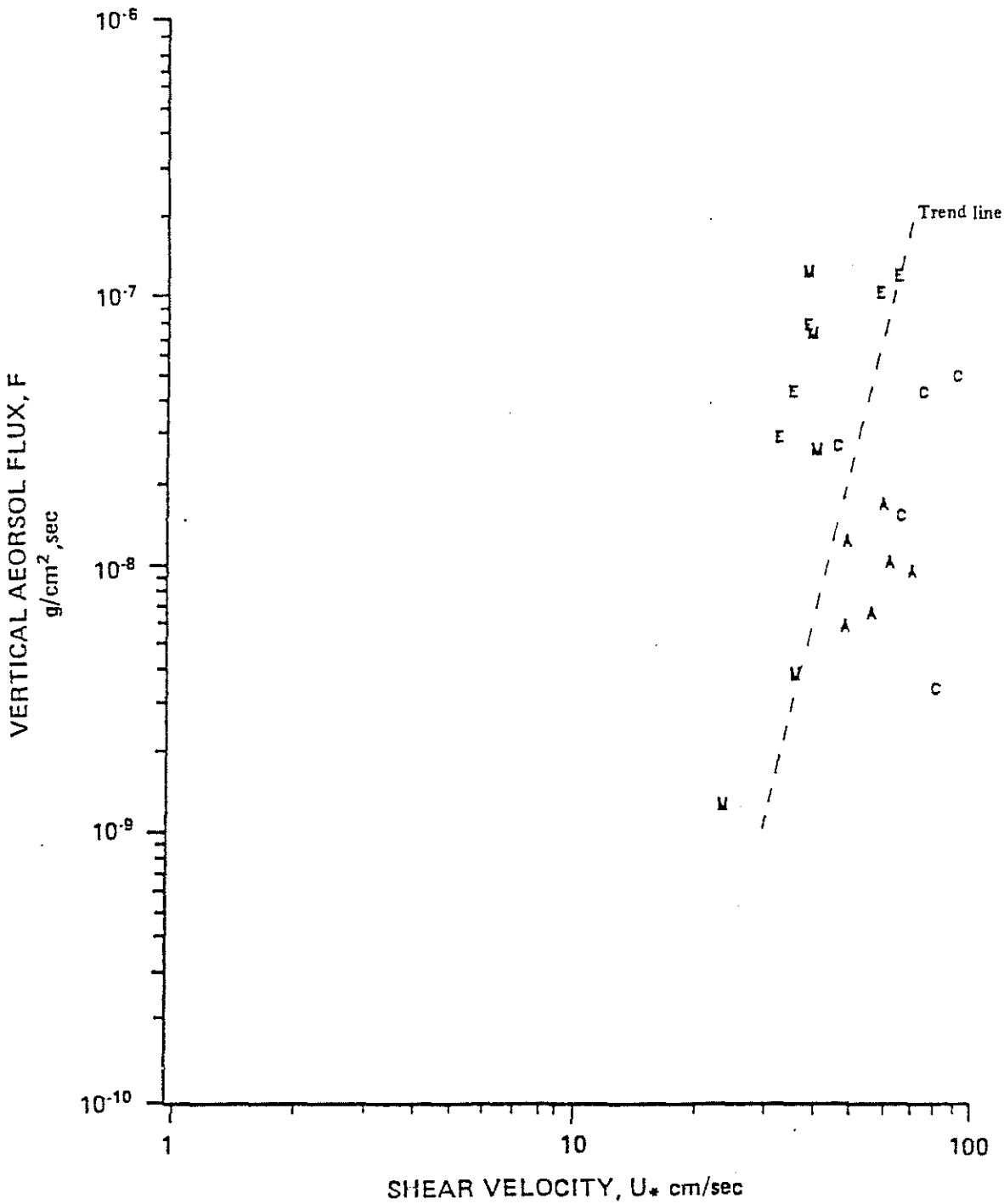

Figure 30

3) Construction sites

$$F = 5.82 \times 10^{-15} U_*^{4.24} \qquad ...22$$

$$r = 0.81 \qquad n = 9$$

4) Mine tailings

$$F = 1.59 \times 10^{-12} U_*^{2.93} \qquad ...23$$

$$r = 0.76 \qquad n = 8$$

The wide data scatter and the lack of a significant correlation coefficient for the agricultural sites again is most likely related to textural and surface parameters (Fig. 30). This is borne out by the fact that significant relationships are present for all individual sites except Maricopa. Although not statistically valid, a trend line has been fitted to the data which can be used for flux estimation:

$$F = 1.445 \times 10^{-18} U_*^{6.026} \qquad ...24$$

In the above relationships, the vertical aerosol fluxes (F) have been expressed as a function of shear velocity (U_*). Similar relationships expressing vertical aerosol flux (F) as a function of wind velocity at 10 m are given in Table 5. The associated wind velocities at 10 m for shear velocities measured in the wind tunnel during each test were computed using the Prandtl formula (eq. 1) and the roughness lengths (z_o) determined from the log height vs wind velocity plots.

Although wind velocity is known to be a major factor in the emission of

TABLE 5

RELATIONSHIP BETWEEN VERTICAL AEROSOL FLUX AND

WIND VELOCITY AT 10 m

All sites	$F = 3.94 \times 10^{-15}\ U_*^{2.28}$	$r = 0.45$
Silt and clay content > 25%	$F = 6.64 \times 10^{-22}\ U_*^{4.490}$	$r = 0.73$
Silt and clay content 15-25%	$F = 3.51 \times 10^{-19}\ U_*^{3.614}$	$r = 0.78$
Silt and clay content < 15%	$F = 1.20 \times 10^{-12}\ U_*^{1.460}$	$r = 0.57$
Natural and Disturbed Desert	$F = 1.78 \times 10^{-16}\ U_*^{2.782}$	$r = 0.71$
Silts developed or modified by fluvial processes	$F = 1.42 \times 10^{-18}\ U_*^{3.377}$	$r = 0.62$
Construction sites	$F = 1.71 \times 10^{-21}\ U_*^{4.355}$	$r = 0.82$
Mine tailings	$F = 7.64 \times 10^{-17}\ U_*^{2.938}$	$r = 0.76$

where F is vertical aerosol flux in g/cm^2 sec
and U is wind speed at 10 m in cm/s

aerosols more detailed research is required to further evaluate surface and textural parameters which directly or indirectly effect the vertical particle flux.

Several authors have suggested that the vertical emission of aerosols is related to the amount of material transported in saltation and creep. The total amount of soil moving in saltation and creep, q (g/cm sec) was measured using a Bagnold type catcher. The data can be fit with the Lettau and Lettau (1978) equation which has the form

$$q = K \cdot U_*^2 (U_* - U_{*t}) \qquad \ldots 25$$

where K is an empirical coefficient with values ranging from 4×10^{-7} for sandy soils to 4×10^{-9} for sandy loam soils.

A horizontal soil flux, q' (g/cm^2 sec) is calculated by dividing the horizontal transport rate (q) by the sediment trap height. The non-dimensional ratio of vertical aerosol flux (F) to horizontal soil flux (q') has been plotted against shear velocity in Fig. 30.

Despite the data scatter a statistically significant trend is apparent. This relationship is expressed by

$$(F/q') = 3.14 \times 10^{-10} U_*^{2.851} \qquad \ldots 26$$

$$r = 0.54$$

A somewhat clearer picture is obtained if the data set is partitioned on the basis of soil texture. The more loamy textured soils (silt + clay > 25%) show a significant increase in flux ratio with increasing shear velocity (fig.31)

RATIO OF VERTICAL SOIL FLUX TO
AVERAGE HORIZONTAL SOIL FLUX

ALL SITES CONSIDERED

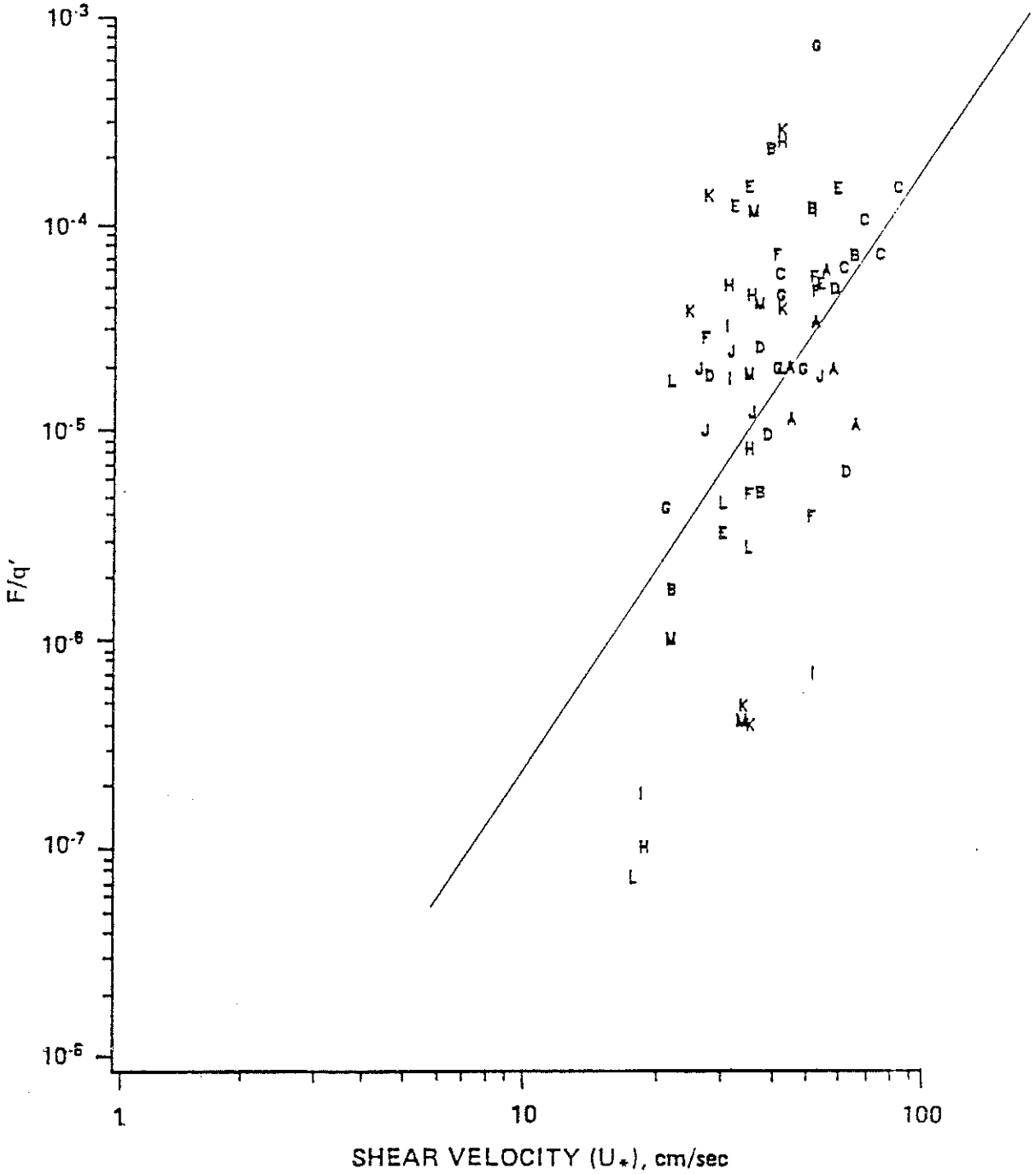

Figure 31

$$(F/q') = 5.01 \times 10^{-12}\ U_*^{4.012} \qquad \ldots 27$$

$$4 = 0.63$$

This result is very similar to that of Gillette (1977) who also found that the flux ratio increased with shear velocity with an exponent of approximately 4.0

Flux ratio curves are also shown for soils with silt and clay contents of 15 - 25% and < 15% in Figs. 32 and 33 respectively. The regression equation for soils with silt and clay contents of 15 - 25% is

$$(F/q') = 3.12 \times 10^{-10}\ U_*^{2.858} \qquad \ldots 28$$

$$r = 0.63$$

and for the sandy soils (silt and clay < 15%)

$$(F/q') = 5.37 \times 10^{-9}\ U_*^{2.101} \qquad \ldots 29$$

$$r = 0.51$$

The weak relationship of vertical flux with shear velocity for the sandy soils shown in Fig. 34 is consistent with the observations of Gillette (1977) who found no significant trend (Fig. 5 in this report).

The above relationships demonstrate the importance of soil texture in the emission of fine particulates. In general, soils with finer textures produced more fine dust per unit horizontal soil flux than the coarser textured soils. In addition, the increase of the exponent value of U_* with increasing percentage of silt and clay indicates that the fine, textured

RATIO OF VERTICAL SOIL FLUX TO
AVERAGE HORIZONTAL SOIL FLUX

GROUPED BY SOIL TEXTURE
SILT AND CLAY > 25%, SITES: B, K, L, M

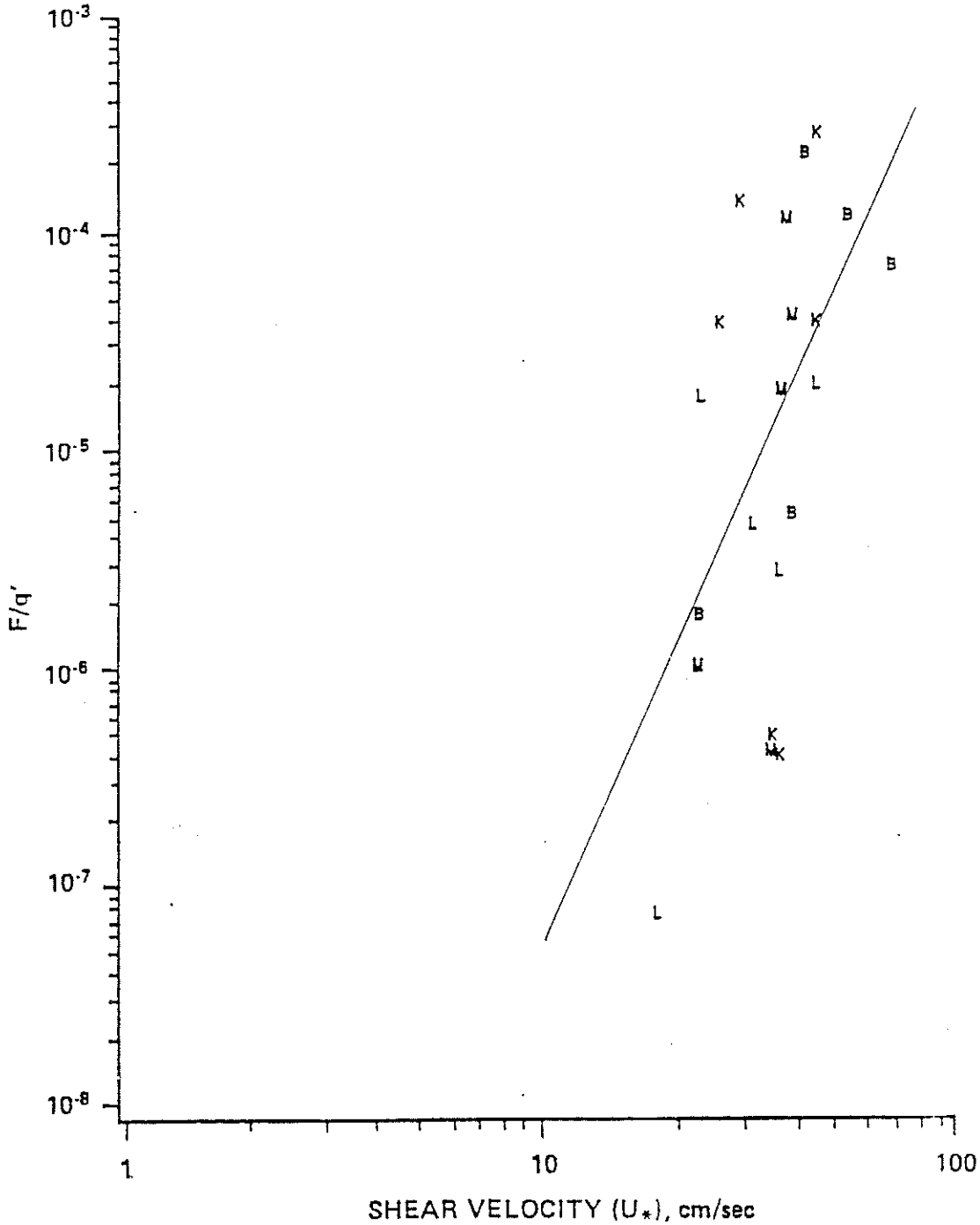

Figure 32

RATIO OF VERTICAL SOIL FLUX TO
AVERAGE HORIZONTAL SOIL FLUX

GROUPED BY SOIL TEXTURE
SILT AND CLAY 15-25%, SITES: A, F, G, H

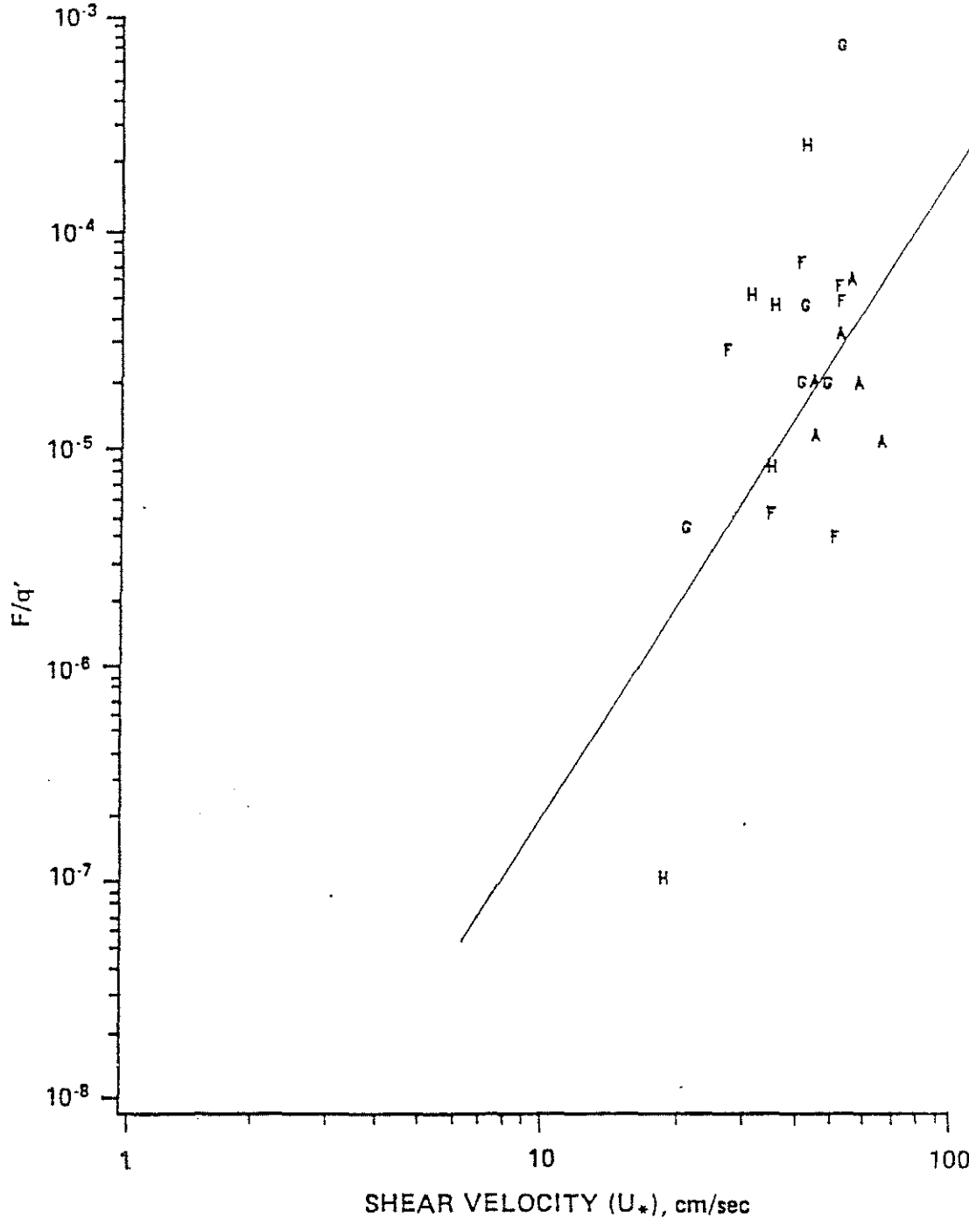

Figure 33

RATIO OF VERTICAL SOIL FLUX TO
AVERAGE HORIZONTAL SOIL FLUX

GROUPED BY SOIL TEXTURE
SILT AND CLAY < 15%. SITES: C, D, E, I, J

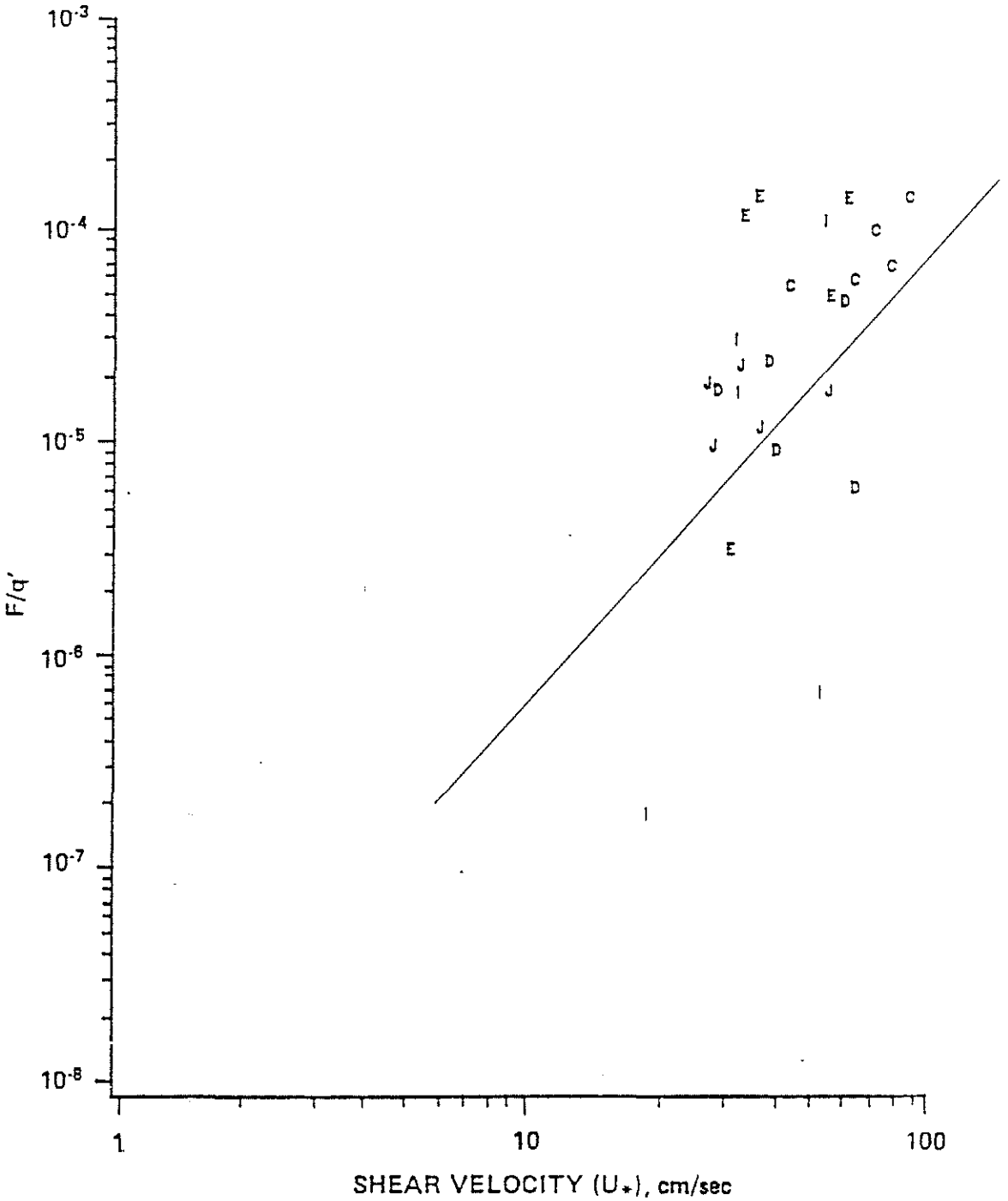

Figure 34

soils produce particulates at a much higher rate as shear velocity increases.

The Nature of the Vertical Aerosol Flux Relationships

All regression equations presented above, relating vertical aerosol flux to shear velocity or wind speed (at 10 m) were derived using the method of least squares. Although all the equations are statistically significant and provide the best fit by the method of least squares, they may not necessarily represent the overall trend of the data as one might expect. This is clearly demonstrated in Fig. 22 which shows the vertical aerosol flux versus shear velocity for all sites. In this plot, the best fit regression line would appear to have a slope which is somewhat greater than would be expected by the overall trend of the data. This situation results from the relatively large data scatter and the fact that both parameters are plotted on a log axis. In regression analysis logging of the parameters and in particular the independent variable, gives greater weight to the smaller values which in some cases results in a fit which seems somewhat anomolous. The situation is exacerbated by large data scatter.

Although not statistically correct a better representation of the data trend might be obtained by fitting a trend line by eye. An 'eye-ball' fit of this nature may in some cases provide a better estimation of the vertical aerosol flux than the statistically correct least squares regression line. This observation should be considered when considering the flux curves present in Figs. 22 to 34. This would also allow for the estimations of emissions for specific surface types (e.g. agriculture).

Aerosol Grain Size Characteristics

Frequency size distirbutions of the aerosols collected during the wind tunnel tests are shown in Table 6. The mean sizes and standard deviations of both the aerosols and the associated surface sediements are also included.

In general, the aerosols are characterized by unimodal size distributions with weak to moderate positive skewness (i.e. tail of coarser grains). The most striking feature of the size distributions is their similarity. Almost all the distributions have modal diameters in the 2.5-10.0 μm size range. The one major exception to this is the Mesa agricultural site which has strong modes in the < 1.0 μm and 1.0 - 2.5 μm size classes reflecting the relatively high silt and clay content (18.6%) of the parent soil (Table 6).

The mean size of the aerosols range from 1.28 to 6.62 μm with a remarkable uniformity of mean sizes. The aerosols are rather poorly sorted with standard deviations ranging from 1.69 to 3.65 μm with the majority being from 3.25 - 3.55 μm. The relatively poor sorting (i.e., flat distributions) of aerosols has also been reported by Gillette et al. (1972), Patterson and Gillette (1977b) and Nickling (1983). It is suggested that the rather poor sorting associated with fine grained aerosols (1-20 μm) results from the low sedimentation velocities of these particles.

Gillette (1977) suggests that since particles have a finite settling velocity (U_{sed}) they must be supported by the upward fluctuations (vertical velocity component) of the wind in order to remain in suspension. Consequently, a particle must have a ratio of approximately one upward to

TABLE 6

GRAIN SIZE CHARACTERISTICS OF SUSPENDED AND SURFACE SEDIMENTS

SITE		GRAIN SIZE DISTRIBUTION OF AEROSOLS (% FREQUENCY)				MEAN SIZE	STANDARD DEVIATION	SHEAR VELOCITY	SURFACE SEDIMENTS MEAN SIZE	SURFACE SEDIMENTS STANDARD DEVIATION
		1.0 μm	1.0-2.5 μm	2.5-10.0 μm	10.0 μm	(μm)	(μm)	(cm/sec)	(μm)	(μm)
MESA AGRICULTURAL	1	24.81	40.88	30.30	4.01	3.31	2.74	62.9	1077.0	1844.0
	2	33.32	34.61	24.01	8.05	3.23	3.04	43.7		
	3	28.96	35.09	28.75	7.20	3.44	3.00	43.4		
	4	48.24	27.20	18.68	5.88	2.59	2.88	50.3		
	5	44.95	31.41	21.91	1.73	2.45	2.52	53.4		
	6	36.78	26.63	28.17	8.42	3.39	3.16	55.5		
GLENDALE CONSTRUCTION	1	42.00	31.68	21.61	4.70	2.72	2.79	22.1	1275.1	2499.0
	2	32.16	37.13	23.68	7.02	3.15	2.95	36.7		
	3	65.53	30.65	1.19	2.63	1.28	1.69	49.4		
	4	17.48	21.33	42.38	18.80	5.15	3.33	62.6		
MARICOPA AGRICULTURAL	1	14.21	23.31	38.76	23.71	5.43	3.41	58.9	749.3	1003.4
	2	24.76	24.92	31.59	18.73	4.55	3.53	66.1		
	3	19.68 31.4	27.30 35.2	38.54 34.7	14.48 / 18.6	4.59	3.281	41.1		
	4	21.46	17.64	35.61	25.28	5.30	3.60	80.1		
	5	27.12	32.68	29.46	10.73	3.78	3.21	72.3		
DISTURBED DESERT, YUMA	1	10.88	15.75	43.46	29.90	6.19	3.27	27.5	591.8	1145.5
	2	14.28	16.79	36.98	31.95	6.01	3.49	38.3		
	3	9.49	21.62	52.69	16.20	5.54	2.97	59.6		
	4	9.42	13.11	45.15	32.32	6.48	3.16	36.6		
	5	14.36	23.81	44.00	17.83	5.19	3.23	55.9		
YUMA AGRICULTURAL	1	17.17	21.54	40.99	20.30	5.21	3.37	29.6	642.6	1686.6
	2	14.03	27.59	44.69	13.69	4.89	3.12	31.9		
	3	14.15	20.41	43.42	22.01	5.50	3.31	34.6		
	4	13.19	20.31	48.16	18.34	5.44	3.16	57.0		
	5	10.91	18.14	46.12	24.83	5.89	3.21	51.7		
ALGODONES DUNE FLATS	1	23.22	23.10	29.55	24.13	4.91	3.67	26.7	2794.0	2819.4
	2	16.15	16.72	41.64	25.49	5.67	3.41	34.3		
	3	13.46	24.45	49.33	12.77	5.04	3.04	50.4		
	4	20.04	32.24	37.74	9.98	4.19	3.11	49.7		
	5	27.42	32.88	25.53	14.17	3.87	3.37	48.7		
	6	10.93	11.20	41.31	36.56	6.62	3.27	40.4		
SCRUB DESERT YUMA	1	46.77	1.74	29.84	21.65	4.37	3.91	50.5	1038.8	1897.4
	2	31.09	30.12	17.18	21.60	4.04	3.72	40.4		
	3	15.09	17.33	44.46	23.12	5.62	3.32	41.3		
	4	23.00	21.33	40.41	15.26	4.69	3.35	46.7		
	5	30.95	23.11	30.92	15.03	4.13	3.47	21.4		

SITE		GRAIN SIZE DISTRIBUTION OF AEROSOLS (% FREQUENCY)				MEAN SIZE	STANDARD DEVIATION	SHEAR VELOCITY	SURFACE SEDIMENTS MEAN SIZE	STANDARD DEVIATION
		1.0 μm	1.0-2.5 μm	2.5-10.0 μm	10.0 μm	(μm)	(μm)	(cm/sec)	(μm)	(μm)
SANTA CRUZ RIVER, TUCSON	1	31.75	29.12	25.36	13.76	3.77	3.39	30.8	1950.7	3251.2
	2	26.99	24.99	33.30	14.72	4.27	3.41	41.7		
	3	6.88	13.31	50.09	29.72	6.53	2.97	34.5		
	4	9.48	20.47	48.61	21.43	5.76	3.10	18.9		
	5	10.78	16.51	47.90	24.82	5.97	3.16	35.1		
TUCSON CONSTRUCTION	1	26.70	36.49	30.74	6.07	3.47	2.92	18.5	1010.9	2001.5
	2	12.36	17.87	45.12	24.64	5.82	3.26	30.9		
	3	22.07	23.80	30.33	23.80	4.94	3.64	30.4		
	4	13.43	18.56	47.11	20.90	5.59	3.21	50.2		
	5	36.71	27.44	23.68	12.16	3.49	3.35	49.1		
AJO, MINE TAILINGS	1	22.15	23.02	35.76	19.07	4.80	3.48	26.8	335.3	202.4
	2	28.68	20.02	30.46	20.84	4.61	3.65	31.2		
	3	16.85	22.75	46.13	14.27	4.96	3.17	25.9		
	5	31.05	27.33	23.22	18.40	4.06	3.60	51.4		
HAYDEN, MINE TAILINGS	1	15.85	22.99	47.10	14.06	5.01	3.14	33.2	271.8	528.3
	2	27.90	22.37	25.85	23.88	4.66	3.75	24.6		
	3	15.64	14.98	33.28	36.10	6.15	3.60	27.5		
	4	14.66	15.33	36.03	33.98	6.11	3.52	41.7		
	5	30.02	26.79	32.72	10.47	3.86	3.25	34.6		
	6	30.35	30.90	21.31	17.44	3.89	3.54	41.7		
SALT RIVER, MESA	1	23.07	10.98	56.75	9.20	4.94	3.04	17.7	398.7	693.4
	2	13.36	16.65	47.16	22.84	5.75	3.23	22.2		
	3	30.05	26.67	22.89	20.39	4.21	3.67	41.7		
	4	9.59	18.62	42.47	29.35	6.11	3.26	34.2		
	5	28.17	24.83	25.78	21.22	4.44	3.68	29.6		
ABANDONED AGRICULTURAL CASA GRANDE	1	25.25	43.73	27.42	3.60	3.14	2.67	36.7	234.4	307.3
	2	32.82	28.19	29.37	9.63	3.59	3.21	22.0		
	3	12.16	16.64	45.60	25.60	5.92	3.25	35.5		
	4	9.31	20.18	50.63	19.88	5.73	3.05	34.5		

downward movements to remain suspended. The probability distribution of the turbulent vertical air velocity is Gaussian with a mean of zero and a standard deviation equal to the shear velocity (Lumley and Panofsky, 1964). Using the non-dimensional ratio U_{sed}/U_*, Gillette (1977) was able to derive an indicator of the upward to downward motions of a particle in air having a normal vertical velocity distribution. For example, a particle with a settling velocity of $U_{set} = 0.4\ U_*$ has a ratio of upward-to-downward movements of 0.5. Since in this case for every upward air movement there are two downward particle movements, the probability that a particle will stay in suspension and rise to any great height is relatively small. Gillette (1974) suggests that particles small than 20 μm are sufficiently small that their sedimentation velocities are usually less than 0.1 U_* for almost all eroding winds and remain in suspension for great distances. Since all particles (< 20 μm) that are ejected into the air stream tend to remain in suspension, the size distributions tend to become more uniform (i.e. poorly sorted) as a result of turbulent mixing regardless of the shear velocity or textural characteristics of the parent soil.

As previously indicated, there is a great similarity in the mean sizes of the suspended sediment despite a considerable difference in the textural characteristics of the surface sediments from which the aerosols were derived. Moreover, no consistent relationship is evident between the mean size and the shear velocity at which the suspended sediments were transported. The lack of consistent relationships between the mean size of aerosols in the 1 - 10 μm size range with shear velocity and textural characteristics of the parent soils has been noted by several authors.

Willeke and Whitby (1975) distinguish three modes or ranges of

particles transported in suspension. The mode involving particles having a mean diameter of the order of 0.01 μm is called the "Transient Nuclei Mode" and is only observed when fresh combustion aerosols are present. This mode has a lifetime of less than one hour. A second mode in the range 0.1 to 1 μm is named the "Accumulation Mode" because it consists mainly of particles which grow from smaller sizes by coagulation or condensation. Particles formed in this manner tend to remain in this size range and have the longest lifetime of any group of particles. The third mode is termed the "Mechanical Aerosol Mode" which occurs in a size range from approximately 1 to 100 μm. Aerosols in this range originate from mechanical processes such as wind blowing over a soil surface, ocean spray, or from mechanically-produced aerosols such as fly ash being introduced into the atmosphere. Because the large particles in this range settle rapidly the number of large particles in the air is highly variable in terms of both maximum size and mass.

Patterson and Gillette (1977a), from their study of aerosols over eroding surfaces, suggest that the distributions are characterized by three distinct modes which may not all be present under a given set of conditions. The authors have labelled the characteristic modes A, B and C. Mode A, which contains a majority of particles having a radius between 1 and 10 μm, is characteristic of soil derived but does not appear to be related to the size distribution of the parent soil from which the aerosols were derived. Mode B is centered between 10 and 100 μm. It is characteristic of the particle-size distribution of the parent soil. This mode is present only under conditions of heavy-to-moderate dust loading. Mode C is centered in the range of radii between 0.02 and 0.5 μm. In general, it is not

related to the other modes in composition or origin but is characteristic of a background aerosol concentration related to the transient nuclei mode of Willeke and Whitby (1975).

Gillette and Goodwin (1974) suggest that mode B is characteristics of particles derived from loose soil aggregates while mode A results from the break-up of aggregates by the saltation process (sandblasting) and the subsequent injection of disaggregated material into the atmosphere. As the wind speed increases over the threshold for erosion, the first particles to be set in motion are those with radii between 20 and 50 μm. The initial movement is primarily due to saltation in which the particles bounce along close to the surface. These particles collide with other particles on the surface, dislodging and disaggregating smaller particles which are injected into the atmosphere and produce mode A. The larger particles which form mode B (10 - 100 μm), quickly settle out because of their high sedimentation velocities. As a result, a relatively narrow range of particle sizes is kept aloft in suspension by the vertical velocity fluctuations.

This selective transport process related to the turbulent nature of most eroding winds would account for the narrow range of mean sizes and poorly sorted distributions associated with samples collected during the wind tunnel tests.

Use of the Wind Tunnel Derived Aerosol Flux Relationships

The vertical aerosol fluxes determined from the wind tunnel tests provide a useful method for the estimation of emissions from various land surfaces. Use of the flux curves reduces the number of assumptions often

made in emission inventories of natural surfaces. An approach to the use of the derived aerosol flux curves is outlined below.

In any given area several different types of surfaces capable of producing aerosols may be present. A common method of delineating and organizing surfaces in emission inventories is the use of grid networks overlaid on detailed maps or airphotographs. Using this procedure the aerial extent and relative position of the various surface types in each grid cell are computed. Although this can be done manually it is much more efficient to use one of the many available mapping programmes that have been developed for the analysis of digitized surfaces (e.g. maps, air photographs). This type of software allows one to identify the various surfaces within a given grid cell as discrete polygons and generate useful parameters (i.e. area, position, centroid) which can be used in subsequent calculations.

Once type surfaces of the study area have been identified it is necessary to estimate the threshold shear velocity or velocity at 10 m that would initiate sediment transport. With some knowledge of the textural, morphological and vegetative characteristics of the surface, thresholds can be determined using the formulae derived from this study or those presented by Gillette et al. (1980).

The most appropriate aerosol flux curve for each surface type is then selected on the basis of the textural and morphological characteristics of the surface. As previously shown two sets of curves have been derived. The first is based on the shear velocities recorded during the wind tunnel tests (Eq. 16 - 24). The second set of equations relate the vertical aerosol flux to the wind velocity at 10 m. These were obtained by estimating the wind

velocity at 10 m using the Prandtl equation (Eq. 1) and the roughness lengths (z_0) recorded during the wind tunnel tests.

Although the velocity at 10 m curves can be used with some confidence there is an inherent error, in that the aerosol flux is more directly related to the shear velocity which itself is a function of the surface roughness. However, to use the shear velocity flux equations, shear velocity must be estimated from the Prandtl equation using standard meteorological wind velocity data which is usually recorded at 10 m. This necessitates the estimation of a characteristic roughness length (z_0). This is commonly done by use of the following expression

$$z_0 = \frac{d}{30} \qquad \ldots 30$$

where d is the average height of the surface protuberances (Bagnold, 1941).

It should be noted that the emission factors derived from the wind tunnel tests provide limiting values for emission rates since they assume an infinite fetch length. Chepil and Woodruff (1957) has shown that the rate of soil movement is zero on the windward or leading edge of an unprotected field and increases with distance downwind until a maximum is reached. He also argues that the distance required for soil flow to reach a maximum on a given soil is the same for all wind velocities and is solely a function of the erodibility of the soil, although Chepil and Woodruff (1957) has shown that limiting fetch distances can be up to several thousand metres for some soils. However, in most cases, maximum flow is reached within a few hundred metres. TRW (1982) in their emission inventory of the Ajo non-attainment area have used a limiting fetch distance of 1000 feet (304.8 m) which is

typical of many non-crusted soils (Craig and Turrelle, 1964). For fetch lengths less than 1000 feet, the fraction of the limiting emission rate achieved is estimated by 1/3 log f, where f is the fetch length in feet.

Estimates of total emissions for any given area can be computed by considering the numerous wind excursions which would occur over the surface in question. For each delineated surface type, in each grid square, the fetch lengths across the surface along the principal compass directions are determined. This would normally be done by running all fetch directions through the centroid of the identified surface unit. This procedure is easily done if appropriate computer mapping software is used in conjunction with a digitized map of the study area.

Following the fetch length determinations a detailed wind velocity distribution for the principal compass directions is established from standard meteorological records. To do this the total duration of winds for a given wind speed class along each principal compass direction is computed (see Table 7). Using the wind speed class mid-point the mean aerosol flux for each class is determined from the appropriate flux curve (Table 5). If the fetch length for a given surface is less than 1000 ft. the computed flux rate (F) is adjusted by the fetch length factor (i.e. (1/3 log f)F). The estimated emission for each wind class is computed by multiplying the adjusted flux rate by the surface area and duration. The total emission for each wind speed class is computed by summing the calculated emission for each principal direction in that class. Total estimated emission for the surface is calculated by summing the emission for each wind speed class.

This procedure is subsequently carried out for each surface type in each grid cell using the appropriate flux curves and fetch corrections. The

total aerosol emission from the total map area is obtained by summing the emissions for all type surfaces in all grid cells.

A hypothetical example for one surface using only the four cardinal directions is shown in Table 7.

TABLE 7

HYPOTHETICAL EMISSION CALCULATIONS

Type of Surface: Scrub Desert

Area of Land Surface: 295,000 m^2 (72.9 acres)

Textural Characteristics: 20% silt and clay
: % aggregates > 0.84 mm = 8%

Wind Regime:

		Wind Speed at 10 m (m/sec)				
		< 6	6-9	9-12	12-15	> 15
Mid Point		(4.5)	(7.5)	(10.5)	(13.5)	(16.5)
Total Hours		7570	580	365	145	35
From:	N	345	50	27	9	3
	E	485	50	54	19	7
	S	790	87	80	22	8
	W	5950	395	204	95	17

Fetch Lengths	Fetch Correction Factors*
N - 800 m	1.00
E - 350 m	1.00
S - 160 m	0.91
W - 825 m	1.00

*Fetch correction factor = 1/3 log (3.281 d)

where d = fetch length in metres

(used if fetch < 305 mm (1000 ft.)).

Threshold Velocity

Assuming 20% silt and clay content and 8% aggregates 0.84 mm, U_{*t} = 30.5 cm/sec (Eq. 14).

continued...

Assuming a logarithmic profile (Eq. 1) and a roughness length (Z_o) of 0.073 the associated threshold velocity at 10 m (U_{10}) = 7.2 m/sec.

Most Appropriate Flux Rate Curve is:

$$F = 3.51 \times 10^{-19}\ U^{3.614} \quad \times \text{ Fetch correction factor if required.}$$

where U is the class mid-point windspeed (cm/sec) (measured at 10 m) if $> U_t$.

Emission for each direction-wind speed class is:

E = F x (Fetch Correction) x Duration (sec) x Area (cm^2)

	Wind Speed (m/sec)				
	6	6-9	9-12	12-15	15
N	Nil	3.66×10^6	8.34×10^6	6.89×10^6	4.75×10^6
E	Nil	4.58×10^6	16.68×10^6	14.56×10^6	11.08×10^6
S	Nil	7.25×10^6	22.49×10^6	15.34×10^6	11.52×10^6
W	Nil	35.26×10^6	63.04×10^6	72.80×10^6	26.91×10^6
		50.75×10^6	110.55×10^6	109.59×10^6	54.26×10^6

Total Emission = 325.15×10^6 g
(= 358 tons)

CITED REFERENCES

Azizov, A., 1977. Influence of soil moisture on the resistance of soil to wind erosion. Soviet Soil Science, Vol. 9, pp. 105-108.

Bagnold, R.A., 1941. The Physics of Blown Sand and Desert Dunes. Morrow, New York, 265 p.

Belly, P.Y., 1964. Sand movement by wind. Tech. Mem. U.S. Army Corps Engs., Coastal Eng. Res. Centre, 38 p.

Brazel, A.J. and Nickling W.G., 1986. The relationship of weather types to dust storm generation in Arizona (1965-1980). J. of Climatology (in press).

Chepil, W.S., 1940. Relation of wind erosion to the dry aggregate structure of soil. Sci. Agric., vol. 21, pp. 488-507.

Chepil, W.S., 1950. Properties of soil which influence wind erosion: I. The governing principle of surface roughness. Soil Sci., vol. 69, pp. 149-162.

Chepil, W.S., 1951. Properties of soil which influence wind erosion: IV. State of dry aggregarte structure. Soil Sci., vol. 72, pp. 387-401.

Chepil, W.S., 1955. Factors that influence clod structure and erodibility of soil by wind: IV. Sand, silt and clay. Soil Sci., vol. 80, pp. 155-162.

Chepil, W.S. and R.A. Milne, 1941. Wind erosion of soil in relation to roughness of surface. Soil Sci., vol. 52, pp. 417-431.

Chepil, W.S. and N.P. Woodruff, 1957. Sedimentary characteristics of dust storms: II. Visibility and dust concentrations. Am. J. Sci., vol. 255, pp. 104-114.

Chepil, W.S. and N.P. Woodruff, 1963. The physics of wind erosion and its control. Advances in Agronomy, vol. 15, pp. 211-302.

Complin, P.G. and P. Piersol, 1978. Uranium mill tailings area fugitive emissions. Proceedings, Third Symposium on Fugitive Emissions Measurement and Control, San Francisco, Ca., October 1978.

Craig, D.G. and J.W. Turelle, 1964. Guide for Wind Erosion Control on Cropland in the Great Plains States. U.S. Department of Agriculture Soil Conservation Service. July 1964.

Deluisi, J., P.M. Furukawa, D.A. Gillette, B.G. Schuster, R.J. Charlson, W.M. Porch, R.W. Feglay, B.M. Herman, R.A. Rabinoff, J.T. Twitty and J.A. Weinman, 1977. Results of a comprehensive atmospheric-aerosol radiation experiment in Southwestern United States. Journal of Applied Meteorology, vol. 15, p. 441.

Gillette, D.A., 1974. On the production of soil wind erosion aerosols having the potential for long range transport. Journal de Recherches Atmospheriques, vol. 8, pp. 735-744.

Gillette, D.A., 1977. Fine particulate emissions due to wind erosion. Trans. ASAE, vol. 80, pp. 890-897.

Gillette, D.A., 1978. A wind tunnel simulation of the erosion of soil: effect of soil texture, sandblasting, wind speed and soil consolidation on dust production. Atmos. Environ., vol. 12, pp. 1735-1743.

Gillette, D.A. and P.A. Goodwin, 1974. Microscale transport of sand-sized soil aggregates eroded by wind. J. Geophy. Res., Vol. 79, pp. 4080-4084.

Gillette, D.A. and T.R. Walker, 1977. Characteristics of airborne particles produced by wind erosion of sandy soil, high plains of west Texas. Soil Sci., vol. 123, pp. 97-110.

Gillette, D.A., I.H. Blifford, Jr. and D.R. Fenster, 1972. Measurements of aerosol size distributions and vertical fluxes of aerosols on land subject to wind erosion. J. Appl. Meteorol., vol. 11, pp. 977-987.

Gillette, D.A., I.H. Blifford, Jr. and D.W. Fryear, 1974. The influence of wind velocity on the size distribution of aerosols generated by the wind erosion of soils. J. Geophy. Res., vol. 78, pp. 4068-4084.

Gillette, D.A., J. Adams, A. Endo, D. Smith and R. Kihl, 1980. Threshold velocities for input of soil particles into air by desert soils. J. Geophy. Res., vol. 85, pp. 5621-5630.

Gillette, D.A., J. Adams, D. Muhs and R. Kihl, 1982. Threshold friction velocities and rupture moduli for crusted desert soils for the input of soil particles into air. J. of Geophys. Res., vol. 87, pp. 9003-9015.

Hagen, L.J. and N.P. Woodruff, 1973. Air pollution from dust storms in the Great Plains. Atmospheric Environment, vol. 7, p. 323.

Idso, S.B. and A.J. Brazel, 1977, Planetary radiation balance as a function of atmospheric dust: climatological consequences. Science, vol. 198, pp. 731.

Iversen, J.D., J.B. Pollack, R. Greeley and B.R. White, 1976. Saltation threshold on Mars, the effect of interparticle force, surface roughness and low atmospheric density. Icarus, vol. 29, pp. 381-393.

Iversen, J.D. and B.R. White, 1982. Saltation threshold on Mars, Earth and Venus. Sedimentology, vol. 29, pp. 111-119.

Leathers, C.R., 1981. Plant components of desert dust in Arizona and their significance for man, in Pewe, T. (ed.), Desert Dust: Origin characteristics and effects on man. Geological Society of America, Special Paper 186, p. 191.

Lettau, K. and H. Lettau, 1978. Exploring the world's driest climate. Institute for Environmental Studies Report 101, University of Wisconsin, Madison.

Lumley, J.L. and H.A. Panofsky, 1964. The Structure of Atmospheric Turbulence. John Wiley and Sons, New York, 239 p.

McKenna-Neuman, C.L., 1984. A combined theoretical and wind tunnel investigation of the effect of capillary water upon the threshold of movement of sand grains by wind, unpublished M.Sc. thesis, University of Guelph, Guelph, Canada, 234 p.

Miller, M.C. and P.D. Komar, 1977. The development of sediment threshold curves for unusual environments (Mars) and inadequately studied material (foram sands). Sedimentology, vol. 24, pp. 709-721.

Nickling, W.G., 1978. Eolian sediment transport during dust storms: Slims River Valley, Yukon Territory, Canada. Canadian J. of Earth Sci., vol. 15, pp. 1069-1084.

Nickling, W.G., 1983. Grain size characteristics of sediment transported during dust storms. J. of Sed. Pet., vol. 53, pp. 1011-1024.

Nickling, W.G., 1984. The stabilizing role of bonding agents on the entrainment of sediment by wind. Sedimentology, vol. 31, pp. 111-117.

Nickling, W.G. and A.J. Brazel, 1984. Temporal and spatial characteristics of Arizona dust storms. J. of Climatology, vol. 4, pp. 645-660.

Nickling, W.G. and M. Ecclestone, 1981. The effect of soluble salts on the threshold shear velocity of fine sand. Sedimentology, vol. 28, pp. 505-510.

Owen, P.R., 1964. Saltation of uniform grains in air. J. Fluid Mech., vol. 20, pp. 225-242.

Patterson, E.M. and D.A. Gillette, 1977a. Commonalities in measured size distribution from aerosols having a soil-derived component. J. Geophy. Res., vol. 82, pp. 2074-2082.

Patterson, E.M. and D.A. Gillette, 1977b. Measurements of visibility vs. mass-concentration for airborne soil particles. Atmos. Environ., vol. 11, pp. 193-196.

Peach, P.A. and L.A. Perrie, 1974, Grain-size distribution within glacial varves. Geology, vol. 3, pp. 43-46.

Perrie, L.A. and P.A. Peach, 1973. Gelatin-coaled microscope slides in sedimentary size analysis. J. of Sed. Pet., vol. 43, pp. 1174-1175.

Péwé, T.L., 1981. Desert dust: an overview. In Desert Dust: Origin, Characteristics and Effect on Man (T.L. Péwé, ed.). Special Paper 186, The Geological Society of America, Boulder, Colorado, pp. 1-10.

Pilat, M.J. and D.S. Ensor, 1971. Comparison between the light extinction aerosol mass concentration relationship of atmospheric and air pollutant emission aerosols. Atmospheric Environment, vol. 5, p. 209.

Prandtl, L. 1932. Meteorologische Anwendung der Stromungslehre. Beitr. Phys. d. Freien Atm., vol. XIX, pp. 188-202.

Schmidt, W., 1925. Der Massenaustauch in Feier Luft und Verwandte Erscheinungen. Henri Grand Verlag, Hamburg.

Shinn, J.H., J.C. Kennedy, J.S. Koval, B.R. Clegg and W.M. Porch, 1976. Observations of dust flux in the surface boundary layer for steady and nonsteady cases. Proceedings, Atmosphere-Surface Exchange of Particulate and Gaseous Pollutants - 1974 Symposium, Richmond, Washington. Energy Research and Development Administration Symposium Series CONF-740921, pp. 625-637.

Willeke, K. and K.J. Whitby, 1975. Atmospheric aerosols: size distribution interpretation. J. Air Pollution Control Association, vol. 25, pp. 529-534.

Wooding, R.A., 1968. A low-speed wind tunnel for model studies in micro-meteorology, 1, General design considerations. Commonwealth Sci. Ind. Res. Organ., Aust. Div. Plant Ind., Canberra City, A.C.T., 1968. Tech. Paper 25, pp. 3-24.